Linköping Studies in Science and Technology
Dissertation No. 1263

CARBON NITRIDE
CHARACTERIZATION AND PROTEIN INTERACTIONS

TORUN BERLIND

Linköping University
INSTITUTE OF TECHNOLOGY

Department of Physics, Chemistry and Biology (IFM)
Linköping University
SE-581 83 Linköping, Sweden

Linköping 2009

During the course of the research underlying this thesis, the author was enrolled in Forum Scientium, a multidisciplinary doctoral program at Linköping University funded by the Swedish Foundation for Strategic Research and Linköping University, Sweden.

Cover: The structure of an albumin molecule (from www.rcsb.org) and an atomic force microscopy surface plot of a graphitic carbon nitride film.

ISBN 978-91-7393-593-7

ISSN 0345-7524

Printed by LiU-Tryck, Linköping 2009

Till De Försummade

Preface

During my career I have followed winding roads. My journey started studying geology, mineral processing and process metallurgy at Luleå University of Technology. I have travelled past material technology and hard materials studied at Sandvik Coromant and the Thin Film Physics Group, and parts of the last years I have spent in the softer area of biochemistry where I have sniffed areas such as protein structure and biomaterials.

The research work presented in this thesis was initialized at the Thin Film Physics Division, and later continued at the Laboratory of Applied Optics, both divisions at Linköping University and the Department of Physics, Chemistry and Biology. The first part of the research was focused on deposition and characterization of carbon-based materials. The second part was a project aimed to investigate the biomolecular interactions with carbon-based materials and also to investigate the process of protein adsorption using *in situ* spectroscopic ellipsometry.

Yet another victim for science

Torun Berlind

Linköping, June 2009

Doubt is uncomfortable, certainty is ridiculous.

Voltaire (French philosopher and writer 1694-1778)

Abstract

This thesis concerns synthesis and characterization of carbon-based materials and the investigation of the possible use, of a selection of these materials, in biomedical applications. Protein adsorption and blood plasma tests were used for this purpose utilizing a surface sensitive technique called spectroscopic ellipsometry.

The materials were synthesized by physical vapor deposition and characterized regarding microstructure, mechanical properties and optical properties. The ternaries B-C-N and Si-C-N as well as carbon and carbon nitrides (CN_x) of different microstructures have been examined. In the B-C-N work, the intention was to investigate the possibility to combine the two materials CN_x and BN, interesting on their own regarding high hardness and extreme elasticity, to produce a material with even better properties. Theoretical calculations were performed to elucidate the different element substitutions and defect arrangements in the basal planes promoting curvature in the fullerene-like microstructure. The Si-C-N ternary was investigated with the consideration of finding a way to control the surface energy for certain applications. Amorphous carbon and three microstructures of CN_x were analyzed by spectroscopic ellipsometry in the UV-VIS-NIR and IR spectral ranges in order to get further insight into the bonding structure of the material.

In the second part of this work focus was held on studies of macromolecular interactions on silicon, carbon and CN_x film surfaces using ellipsometry. One purpose was to find relevance (or not) for these materials in biological environments. Materials for bone replacement used today, e.g. stainless steel, cobalt-chromium alloys and titanium alloys suffer from corrosion in body fluids, generation of wear particles in articulating systems, infections and blood coagulation and cellular damage leading to impaired functionality and ultimately to implant failure. Artificial heart valves made of pyrolytic carbon are used today, with friction and wear problems. Thus, there is still a need to improve biomaterials. The aim of the fourth paper was to investigate the interaction between carbon-based materials and proteins. Therefore, amorphous carbon (a-C), amorphous (a), graphitic (g) and fullerene-like (FL) CN_x thin films were exposed to human serum albumin and blood plasma and the amount of protein was measured *in situ* using spectroscopic ellipsometry. Surface located and accessible proteins after blood plasma incubations were eventually identified through incubations in antibody solutions.

Antibody exposures gave indications of surface response to blood coagulation, complement activation and clotting. The a-C and FL-CN_x films might according to the results have a future in soft tissue applications due to the low immuno-activity, whereas the g-CN_x film possibly might be a candidate for bone replacement applications.

"Layered" structures of fibrinogen, a fibrous but soft protein involved in many processes in our body, were grown *in situ* and dynamically monitored by ellipsometry in order to try to understand the adsorption process and molecule arrangement onto a silicon surface.

In the last paper of this thesis, the effects of ion concentration and protein concentration on the refractive index of water-based solutions used in *in situ* ellipsometry measurements were demonstrated and spectral refractive index data for water solutions with different ionic strengths and protein concentrations have been provided.

POPULÄRVETENSKAPLIG SAMMANFATTNING

Sedan urminnes tider har nya material fascinerat mänskligheten och varit en av grundstenarna för utvecklingen av vårt samhälle som det ser ut idag. Utvecklingen är ständigt pågående, och ända sedan bronset och järnet började användas av människan, fram till dagens sofistikerade utveckling och förbättring av material såsom; halvledare för elektronik; stålsorter; keramer för rymdskyttlar; smarta polymerer; material i verkstadsindustrin; och sist men inte minst; nya material som används i människokroppen - så kallade biomaterial -, har människans nyfikenhet varit den stora drivkraften. Denna avhandling fokuserar på delar av en materialgrupp - kolbaserade material - som har blivit viktig i en mängd olika applikationsområden och som troligen fortfarande har möjligheter att hitta nya användningsområden.

Till kolbaserade material, som varit en av grundstenarna för det här arbetet, hör bl.a. hårda och nötningsbeständiga material i form av t.ex. diamantlikt kol, amorft kol och fullerenlik kolnitrid. En annan form av kolbaserade material är friktionsfria (smörjande) material i form av t.ex. grafit, och en tredje klass är kolbaserade biokompatibla komponenter som t.ex. pyrolytiskt kol.

Kol som alltså är en viktig komponent i många av vardagens material, förutom ovanstående exempel även plast och stål, är också en av de viktigaste byggstenarna för liv eftersom det ingår i proteiner som är uppbyggda av aminosyror vars sidokedjor huvudsakligen har centrala delar uppbyggda av kol. Detta är en av tankarna bakom forskningen om möjligheterna att använda kolbaserade material i människokroppen. Så enkelt är det dock inte. Bara för att samma element som ingår i ett material också finns naturligt i kroppen, så behöver det nödvändigtvis inte accepteras av kroppen utan problem. Det är mycket som spelar in i interaktionen mellan mänsklig vävnad och ett "främmande" material. Till att börja med har ytans morfologi en stor inverkan liksom ytans laddning och energi samt molekylära ytgrupper, Sådana egenskaper är inte alltid så lätt att förändra utan att materialets övriga egenskaper förändras.

Beroende på vilken applikation ett material är tänkt att användas i kan exempelvis nötningsbeständighet för benkontakterande material nämnas som en viktig parameter samt en ytas förmåga att *inte* trigga kroppens naturliga försvar mot främmande material i

form av koagulation och aktivering av immunsystemet. Med detta som bakgrund har studier dels utförts i form av karaktärisering av olika former av kolbaserade material som CN_x, BCN och SiCN, dels i form av proteinadsorptionsstudier både med modellsystemet fibrinogen på kiselytor samt med albumin som modellprotein på CN_x och amorfa kolfilmer. I denna avhandling har dels själva kolnitridytorna och dels det dynamiska förloppet av proteinmolekylers adsorption till olika ytor kunnat studeras med hjälp av en teknik som kallas ellipsometri. Denna teknik bygger på att polarisationen hos ljus förändras vid reflektion mot en materialyta och kvantitativt kan analyseras före och efter denna reflektion samt därefter användas för bestämning av bl.a. tjocklekar och brytningsindex för materialet ifråga.

Inledande studier med exponering av amorft kol, amorf, grafitlik och fullerenlik kolnitrid för albumin och blodplasma samt identifiering av ytlokaliserade och tillgängliga proteiner efter plasmainkubationen genom inkubering i antikroppslösningar visar indikationer på ytrespons för blodkoagulation, komplementaktivering och klottning i varierande grad för dessa material. Den amorfa och den fullerenlika kolnitriden skulle med avseende på resultaten kunna ha en framtid i applikationer för mjukvävnad då dessa filmer uppvisar låg immunaktivitet. Den grafitlika kolnitriden skulle kunna vara en kandidat för benkontakterande applikationer.

För att bättre förstå adsorptionsprocessen då ett protein adsorberar på en yta växtes lagrade strukturer av fibrinogen, ett fibröst men mjukt protein som är involverat i många av kroppens biokemiska processer, samtidigt som förloppet följdes *in situ* med ellipsometri.

PAPERS INCLUDED IN THE THESIS

I. Microstructure, mechanical properties, and wetting behavior of Si–C–N thin films grown by reactive magnetron sputtering, Torun Berlind, Niklas Hellgren, Mats P. Johansson, Lars Hultman; *Surface and Coatings Technology 141 (2001) 145-155*

II. Fullerene-like B-C-N thin films: a computational and experimental study, Niklas Hellgren, Torun Berlind, Gueorgui Gueorguiev, Mats P. Johansson, Sven Stafström, Lars Hultman; *Materials Science and Engineering B 113 (2004) 242-247*

III. Spectroscopic ellipsometry characterization of amorphous carbon and amorphous, graphitic and fullerene-like carbon nitride thin films, T. Berlind, A. Furlan, Z. Czigany, J. Neidhardt, L. Hultman, H. Arwin; *Thin Solid Films, In press*

IV. "Protein adsorption on thin films of carbon and carbon nitride monitored with ellipsometry", T. Berlind, M. Poksinski, L. Hultman, P. Tengvall, H. Arwin; *Manuscript in final preparation*

V. "Formation and cross-linking of fibrinogen layers monitored with *in situ* spectroscopic ellipsometry", Torun Berlind, Michal Poksinski, Pentti Tengvall, Hans Arwin; *Submitted to Colloids and Surfaces B:Biointerfaces*

VI. Effects of ion concentration on refractive indices of fluids measured by the minimum deviation technique, T. Berlind, G. K. Pribil, D. Thompson, J. A. Woollam, H. Arwin; *Physica Status Solidi (c) 5 No. 5 (2008) 1249-1252*

CONTRIBUTION TO INCLUDED PAPERS:

I. I was responsible for the planning, did all experimental work except HRTEM and XPS, took part in RBS measurements, and was responsible for all analyses. I wrote the first draft of the paper and was responsible for the iterative process to the final version.

II. I was involved in planning, did all experimental work except HRTEM and the theoretical ab initio calculations. I took part in RBS measurements and made the analyses. I contributed to the writing.

III. I was responsible for the planning, did all experimental and analytical work (except HRTEM) excluding the film deposition that was performed together with J. Neidhardt and A. Furlan. I wrote the first draft of the paper and was responsible for the iterative process to the final version.

IV. I was responsible for the planning, did all experimental work and analysis, and wrote the first draft of the paper.

V. I was involved in planning, did all experimental work and analysis, wrote the first draft of the paper and was responsible for the iterative process to the final version.

VI. I was involved in planning, did all experimental work and analyses, wrote the first draft of the paper and was responsible for the iterative process to the final version.

PAPERS RELATED TO THE THESIS

I. "Structure of DC-sputtered Si-C-N thin films", G. Radnóczi, G. Sáfrán, Zs. Czigány, T. Berlind, L. Hultman; *Thin Solid Films, 440 (2003) 41-44*

II. "Mechanical and tribological properties of CN_x films deposited by reactive magnetron sputtering", E. Broitman, N. Hellgren, O. Wänstrand, M.P. Johansson, T. Berlind, H. Sjöström, J.-E. Sundgren, M. Larsson, L. Hultman; *Wear, 248 no. 1-2 (2001) 55-64*

III. "Growth of CN_x/BN:C multilayer films by magnetron sputtering", M.P. Johansson, N. Hellgren, T. Berlind, E. Broitman, L. Hultman, J. -E. Sundgren; *Thin Solid Films, 360 (2000) 17-23*

IV. "Design, plasma studies, and ion assisted thin film growth in an unbalanced dual target magnetron sputtering system with a solenoid coil", C. Engström, T. Berlind, J. Birch, L. Hultman, I.P. Ivanov, S.R. Kirkpatrick, S. Rhode; *Vacuum, 56 (2000) 107-113*

List of abbreviations

a	amorphous
AFM	atomic force microscopy
APTES	3-aminopropyltriethoxysilane
C	compensator angle
C3c	complement component 3c
d	thickness
dn/dc	increments in refraction with concentration
EDC	ethyl-3-dimethyl-aminopropyl-carbodiimide
Fib	fibrinogen
FL	fullerene-like
HMWK	high molecular weight kininogen
HSA	human serum albumin
I	ionic strength
IgG	immunoglobulin G
k	extinction coefficient
L	the interaction length
Milli-Q	ultrapure filtered water
n	refractive index
N	complex refractive index
NE	null ellipsometer
NHS	N-hydroxysuccinimide
p	parallel to the plane of incidence
P	polarizer angle
PBS	phosphated buffered saline
pI	isoelectric point (net zero charge)
QCM	quartz crystal microbalance with dissipation
RBS	Rutherford back scattering spectrometry
Rp	complex reflection coefficient for p-component
Rs	complex reflection coefficient for s-component
s	perpendicular to the plane of incidence (from *senkrecht*)
SBF	simulated body fluid
SE	spectroscopic ellipsometer
SEM	scanning electron microscopy
TEM	transmission electron microscopy
UV-Vis	ultraviolet-visible
XPS	X-ray photoelectron spectroscopy
Γ	adsorbed amount
δ	phase difference
Δ	ellipsometry angle, phase difference
λ	wavelength of light
ρ	ratio of *Rp* and *Rs*
Φ	angle of incidence
Ψ	ellipsometry angle, amplitude

Contents

Chapter 1

Introduction

During all times new materials have fascinated humanity and have been part of the foundation for the development of the human society. The development is still ongoing, and ever since the birth of bronze and iron, until today's sophisticated amendment and development of materials as e.g. electronics and steel qualities, and the discovery of new materials like ceramics for space vehicles, materials in engineering and tooling industry, smart polymers and last but not least new materials for the use in the human body - so called biomaterials -, the human curiosity is the most important driving force. This thesis focuses on parts of a group of materials that has become important in a wide range of application areas, and still there is a belief that these materials will find new applications. This chapter gives a short introduction to carbon nitride based materials and the research objectives of the work presented in the thesis.

1.1 Research objectives

The aims of the research behind this work were several and resulted in a quite broad work including deposition and characterization of carbon nitrides, the use of a few techniques for testing of biocompatibility and/or bioactivity and the use of an optical method called ellipsometry to monitor protein adsorption and characterize carbon nitride.

In the initial projects of my work, the objective was to explore of the *effects of doping of carbon nitride* (CN_x) matrices, resulting in the ternaries B-C-N and Si-C-N and the characterization of these materials.

Carbon nitrides have been characterized rather extensively during the last decades regarding microstructure, bonding configuration, tribological and electrical properties using a wide variety of measurement techniques. However, the correlation between *spectroscopic ellipsometry* data and microstructural bonding configurations has been sparingly examined and data are rarely available in the literature. The later projects were focused on *protein adsorption* and it was used as a simple tool for testing of *potential biomaterials* by exploring the interaction of biomolecules with carbon-based materials. Furthermore, proteins were adsorbed into thick protein layers. The aim of this was to dynamically as well as at steady-state characterize the *structure of the protein layer* and possibly also determine the orientation of the protein molecules. The application of thick layers of protein are of interest in several areas e.g. as a matrix for incorporation of drugs for slow release in the body and in sensor technology. The need for a refractive index of water with ions in the ellipsometric analyses of these protein adsorption studies urged us to measure the dependence of refractive indices of fluids with ions and protein molecules using the minimum deviation technique.

1.2 Outline

This thesis consists of three major parts with the following main themes. The first part, presented in Chapter 2, deals with growth and characterization of carbon-based materials, especially CN_x, and the ternaries Si-C-N and B-C-N. The second part (Chapter 3) covers macromolecular interactions regarding protein adsorption and a brief description of some methods to monitor proteins sticking to a surface. Ellipsometry, the method used in this part of the work, will be discussed in more detail in Chapter 4, the third part of the thesis. This will be followed by a summary of the results of appended papers in Chapter 5 and by way of conclusion an outlook is presented. Results are presented in the form of published or submitted papers appended to the thesis. Papers I to III cover growth, microstructure and properties of the three groups of materials dealt with in the thesis; Si-C-N, B-C-N and CN_x, respectively. Papers IV and V cover adsorption of proteins onto CN_x and Si surfaces.

The last paper is a work performed together with J.A. Woollam Company Inc. and demonstrates the effects of ion concentration and protein concentration on the refractive indices of fluids.

Chapter 2

Carbon-based materials

In this chapter a short introduction to carbon, carbon nitrides and the carbon-nitride-based ternaries is given, followed by a discussion of bonding configurations and microstructure of these materials. The deposition technique used for the film growth is presented and the most important analyses methods are discussed. The section is concluded with a short overview of carbon-based materials in medical applications.

2.1 Carbon

If we are contemplating our surroundings it soon makes us realize that a majority of the material is based on carbon. Carbon is an element of importance in a wide range of areas covering the most important elements for life, as a constituent of the building blocks in our bodies - the amino acids - as well as being an important element in the "material world" in the form of steel and other hard materials as well as polymers, ceramics, pyrolytic carbon, to mention a few. Amorphous carbon, tetrahedral carbon, diamond-like hydrogenated carbon, synthetic diamond, fullerenes, CN_x, graphene, carbon nanotubes, graphane; the list of new or different structures based on carbon grows for each year due to the extensive research and discovery of

new carbon-based materials. A lot of work has been performed in finding carbon-based materials with certain physical and chemical properties suited for a particular application and numerous of papers have been produced on theoretical calculations, synthesis, characterization and properties of these materials. The interest is due to that the carbon atom is small and has the ability to form covalent bonds and form a matrix with dense structure, and therefore is an excellent constituent in the hunt for hard compounds. The carbon-based group of materials has met a new era in nanotubes (rectangular sheets of graphene rolled-up to hollow cylinders) and the recently discovered graphane, a structure in which a hydrogen atom is bonded to each of the carbon atom in the graphene sheet [1]. The graphane sheet has insulating properties instead of being highly conductive as is graphene.

2.2 Carbon nitrides

In the beginning of the "carbon nitride era" numerous of papers were written about β-C_3N_4, the hypothetical compound predicted by Liu and Cohen [2,3] to have a bulk modulus of 427 GPa, which is a value close to that of diamond (443 GPa). In addition four other structures of crystalline CN have been predicted, e.g. α-C_3N_4, which is an iso-structural phase to the more well-known α-Si_3N_4. While the evidence for the existence of the C_3N_4 compounds remains to be proven, CN_x has been deposited in different structures and compositions, as e.g. amorphous[1], graphitic[2], turbostratic[3] and "fullerene-like"[4], using a variety of deposition techniques and the mechanical, electrical and optical properties, as well as detailed structures of these materials have been examined by many groups.

The effect of introducing nitrogen into the amorphous or graphite-like carbon matrix is that it induces curvature into the structure, with bent and intersecting basal graphite planes as a result. The fullerene-like microstructure has become of certain interest, because of the elastic behavior in combination with a high hardness which is

[1] An amorphous structure is here denoted as a material with no apparent ordering or crystallinity when imaged in high-resolution microscope and with very low or insignificant scattering of X-rays.
[2] A graphitic structure denotes a material mainly consisting of graphitic domains with less curvature as compared to the fullerene-like structure.
[3] The turbostratic structure is similar to graphite, but the basal planes are randomly rotated around the c-axis, and thus do not exhibit a regular ABAB… stacking sequence as do graphite.
[4] A "fullerene-like" structure is attributed to curved and bent graphite sheets intersected by sp^3 hybridized carbon forming a three dimensional structure with smaller domains and a more pronounced curvature as compared to the graphitic structure.

of great importance in certain applications. Hardness values for carbon nitride (CN_x) have been reported in the range 10-40 GPa depending on microstructure and deposition technique [4-6].

So, even though the dream of producing a material with a bulk modulus close to diamond so far is not fulfilled, the research on carbon nitrides seem to continue due to the fact that these materials exhibit a wide range of optical, electrical and mechanical properties that perhaps open possibilities for new applications.

2.2.1 Carbon nitride compounds

New applications and higher demands of the materials involved, promote the research for new materials. In this never ending search for new materials, all possible combinations of elements, structures and properties are performed with the expectation of finding a material with improved and/or new properties. Research on material from ternaries and quaternaries has in this respect been of great importance and a continued work is needed. Successful research has already been devoted to the ternary Ti-C-N, where the hard materials TiN and TiC have been combined into a new material. Another group of materials, with increasing importance are the so called $M_{n+1}AX_n$ phases (n=1, 2, 3), where M, A, and X denote an early transition metal, an A-group element, and carbon/nitrogen, respectively. These phases (e.g., Ti_2AlN, Ti_3SiC_2) form a family of nano-laminated ternary carbides and nitrides of great importance due to their combined metallic and ceramic properties. [7]

With the expectation of finding a material with enhanced and/or combined properties compared to the binaries of these materials, compounds within the ternaries B-C-N and Si-C-N have been examined in this study.

2.2.1.1 Si-C-N

The research on Si-containing carbon-based materials and the ternary Si-C-N was very limited up to about a decade ago and was mainly focused on mechanical properties [8,9], although in some work also electrical and optical properties have been evaluated [10,11]. During the last 10 years the number of published papers have increased but most of the work has concerned chemical vapor deposited (CVD) films, being amorphous, or consisting of crystalline phases of Si_3N_4, SiC_x, SiN_x or solid

solutions of SiCN [12,13]. The surface characteristics regarding wettability of Si-doped CN-networks have so far only been studied to a limited extent, e.g. Grieschke *et al.* studied Si-doped a-C:H networks [14].

2.2.1.2 B-C-N

Graphite, diamond-like carbon, hexagonal BN and cubic BN are all important materials in mechanical applications, compounds that consist of the elements boron, carbon and nitrogen, three neighboring elements in the periodic table. The phase diagrams of BN and C are similar with a hexagonal structure at ambient temperature and a hexagonal (wurtzite) as well as a cubic (zinc blend) form at higher temperatures and pressures. These similarities have been a motivation for the synthesis of the ternary phase BCN for the last three decades. In addition, the hexagonal phase of BN (h-BN or t-BN, the so-called hexagonal or turbostratic BN with sp^2 bonding and a graphitic or turbostratic structure) thin films have shown to exhibit similar microstructures compared to C and CN_x. The focus has been (as for carbon) on the cubic phase of the BN, whereas the synthesis and characterization of the hexagonal phase have been ignored.

Compared to the ternary Si-C-N there is a larger number of papers written about BCN materials. Most of the materials have been grown by CVD and mixed phases of BN and C are commonly reported, whereas also solid solutions of ternary BCN compounds might exist [15,16]. Besides the excellent lubricating properties of graphite and h-BN, amorphous structures within the B-C-N triangle can exhibit high hardness values, up to 35 GPa [17,18].

2.3 Microstructure

2.3.1 Carbon and nitrogen bonding configurations

Both carbon and nitrogen are able to form covalent bonds with other atoms. They have a similar distribution of valence electrons with partly filled 2p orbitals. Carbon, with the electronic configuration $1s^2 2s^2 2p^2$, has four valence electrons and the ability to form three hybridization states enabling also three major bond configurations, namely sp^3 tetrahedral bonds (only σ bonds), sp^2 planar graphite-like bonds

(3σ and 1π) and the sp linear triple bond (2 σ and 2 π). In the sp^3-hybridization (as in diamond) each valence electron forms a σ-bond, and since the orbitals are identical they are evenly distributed in space in a tetrahedral manner as seen in Figure 2.1. The three electrons in the sp^2 configuration (as in graphite) appear instead in a trigonal manner forming strong intra-layer σ bonds. The remaining 2p electron lies in a π orbital, perpendicular to the bonding plane, and forms a weak π-bond with neighboring π orbitals. The electrons in a π orbital can be delocalized and form resonance structures of single and double bonds in appropriate matrices. In the sp-hybridization (as in acetylene) two electrons form σ bonds and two electrons are placed in the π orbitals forming π bonds.

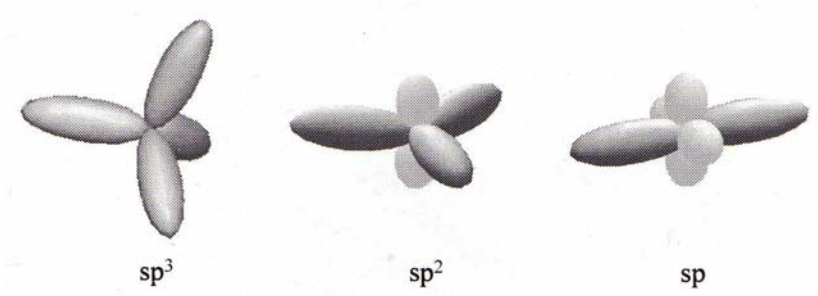

Figure 2.1: Schematic illustration of three possible types of electron orbital hybridization for carbon; sp^3 tetrahedral bond (diamond), sp^2 planar graphite-like bond (graphite) and sp linear triple bond (alkyne). The darker (longer) atomic orbitals are the hybrids that form σ-type molecular orbitals, whereas the lighter (smaller) atomic orbitals are the remaining 2p electron(s) that form π-type molecular orbitals. (From Ref. [19]).

The nitrogen electronic configuration is $1s^2 2s^2 2p^3$, giving 5 valence electrons. The valence electrons show bond hybridizations similar to carbon, see Figure 2.2. The nitrogen atom also hybridizes in the sp^3 arrangement, but differs from carbon due to that there is a "lone pair" of electrons left on the nitrogen that does not participate in the bonding. The angle between the three σ-bonding orbitals is therefore slightly deflected to 109° compared to 107° in diamond. Two possibilities are present for the sp^2-hybridization of nitrogen as the fifth valence electron will cause a two-fold or a three-fold coordination. In the case of three-fold coordination (as carbon in graphite) the extra electron will form a lone pair with the remaining unhybridized 2p orbital and

the atom will be left with three σ bonds and a non-bonding lone pair in a planar configuration. This configuration is referred to as nitrogen in a substitutional graphite site. In the two-fold coordination only two sp^2 hybrid orbitals will form σ bonds whereas the fifth valence electron will form a non-bonding lone pair with a sp-hybrid orbital and the remaining 2p orbital may participate in π-resonance structures with other atoms. This configuration is referred to as pyridine-like.

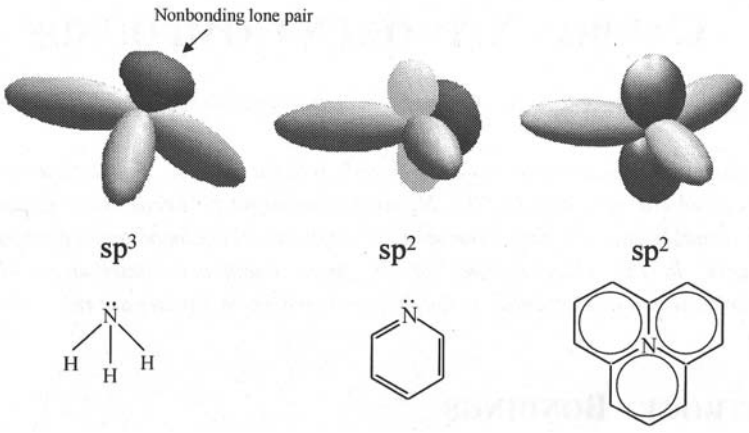

a) b) c)

Figure 2.2: Schematic illustration of three possible types of electron orbital hybridizations of nitrogen with corresponding Lewis structures for representative compounds. a) sp^3 hybridization (as in ammonia), b) two-fold coordinated sp^2-hybridization (as in pyridine) and c) three-fold coordinated sp^2 hybridization (as N in a substitutional graphite site) The fifth valence electron is paired with either a hybrid orbital (as in a) and b)), or with the remaining $2p_z$ electron (c)), and form a lone pair, represented by the darkest orbital. In the Lewis structure this is represented by two dots. (From Ref. [19]).

2.3.2 Graphite, graphene, fullerenes and the fullerene-like microstructure

The most common allotropes of pure crystalline carbon are graphite and diamond, having a hexagonal and a cubic crystal structure, respectively. More unordered structures of carbon as well as CN_x are the amorphous and turbostratic structures. The turbostratic structure is similarly to graphite build up of graphene sheets, but the

sheets are randomly rotated around the c-axis, causing the spacing between planes to be greater than ideal [20]. The fullerene-like (FL) microstructure is another type of structure that evolves when nitrogen is added into the graphene sheets, making them bend and buckle due to the formation of pentagons (Figure 2.3).

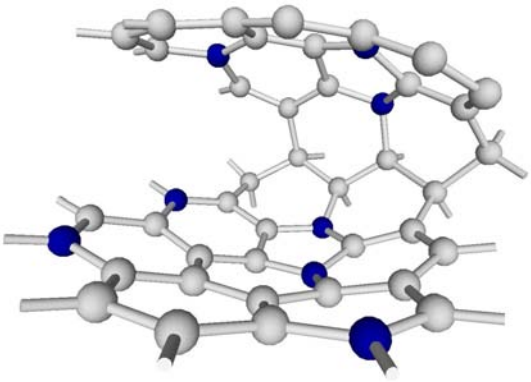

Figure 2.3: Pentagon incorporation in the hexagonal structure gives a bent and intersecting feature of the graphene sheets. C atoms are grey and N atoms are black in the schematic figure (From Ref. [4]).

Gueorguiev et al. have theoretically shown that the bending of a graphene sheet is more likely when the nitrogen concentration in the films exceeds 17.5 at.%, since at higher concentrations it is energetically more favorable with double pentagon defects which induce curvature to a higher extent as do a single pentagon defect. At lower concentrations only isolated pentagons are expected leading to a limited curvature [21].

The origin of the intersections is, however, still discussed in literature. It is suggested that the sheets are intersected by sp^3 hybridized carbon forming a three dimensional structure with smaller domains and a more pronounced curvature as compared to the graphitic structure leading to a highly resilient material. Gammon [22] e.g., has by initial calculations shown that nitrogen bonded in a pyridine-like manner might induce cross-linking if a concurrent presence of a vacancy defect exists nearby, resulting in an out-of-plane nucleation site where three-dimensional growth can be initiated without sp^3-C bonds. Based on theoretical calculations, Gueorguiev et

al. similarly suggested that nitrogen might induce bond rotation at a nitrogen atom in a substitutional site for carbon in the graphene sheet which can result in a simultaneous pentagon formation and cross-linkage between the planes (Figure 2.4) [21].

FL structures shall not be confused with fullerenes, which are ball-like closed-cage carbon structures with 28 up to 540 carbon atoms, with 60 atoms for the most known fullerene-molecule, the "Buckyball" discovered in 1985 [23].

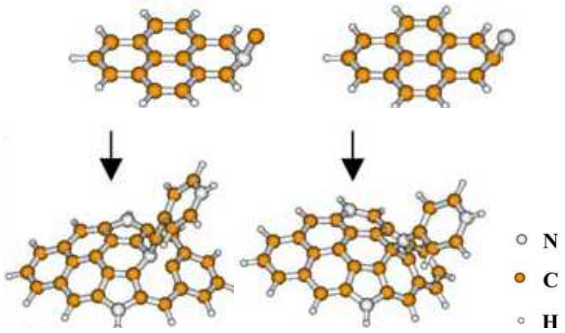

Figure 2.4: Schematic representation of a nitrogen induced bond rotation with simultaneous pentagon formation and cross-linking. To the left, a carbon atom is arriving and bonded to a peripheral nitrogen atom in the graphene sheet, and to the right a nitrogen atom is added to a graphene sheet. From reference [21].

As already mentioned in the beginning of this chapter, numerous of structures of carbon based materials have been described during the years and it seems that different names sometimes have been used for the same type of material and vice-versa. For example, the name diamond-like carbon (DLC) is often used for both tetrahedral carbon (ta-C) and hydrogenated amorphous carbon (a-C:H), where the latter, by some authors, is suggested to belong to the group of diamond-like hydrogenated carbon (DLHC) [24]. In addition, the transition between the different groups of structures seems to be floating, e.g., the transition between microstructures of the amorphous and graphitic forms of CN_x, as well as the transition between graphitic and FL forms are often floating. Apparently, some confusion still exists in the terminology and classification of carbon-based materials. In this thesis the

microstructure of the films are limited to be non-hydrogenated and mainly sp^2-bonded thin films.

In the case of SiCN-films in paper I, both amorphous, graphitic and FL microstructures as well as amorphous microstructures with embedded nano-crystals have been recognized. The BCN-films (Paper II) all exhibited a FL microstructure, whereas the CN_x-films in Papers III and IV had either an amorphous, graphitic, or FL microstructure.

2.4 Deposition of carbon-based films

Several techniques are used for the growth of thin films of carbon compounds. A variety of chemical vapor deposition techniques (CVD) (conventional or plasma enhanced), laser ablation, arc evaporation, and magnetron sputtering have been used resulting in a wide variety of film microstructures. Reactive unbalanced direct current (d.c.) magnetron sputtering was used as deposition technique for the films grown in this work. The advantage with d.c. magnetron sputtering is the possibility to control and vary plasma parameters and the possibility of low temperature growth. Thus, film deposition onto temperature-sensitive substrates, such as martensitic steel or light metal alloys, can be made by these techniques. For other deposition processes operating at elevated temperatures, these kinds of substrate materials may undesirably undergo phase transformations or microstructural changes.

The magnetron sputtering process can simply be described as evaporation of material from a target (cathode) source, transportation of the material through a gas plasma in a vacuum chamber to a substrate surface, and a final condensation on the substrate. In a d.c. discharge a potential is applied to the target (typically ~500V) and a noble gas is introduced to the vacuum chamber. Ionized gas atoms are accelerated towards the most negative electrode, the target, and cause a collision cascade of sputtered atoms, secondary electrons and reflected ions and neutrals. A magnetic field from magnets behind the target is applied in order to trap the electrons close to the target surface and hence increase ionization of the sputtering gas. This is referred to as magnetron sputtering. If the process is carried out in a discharge containing a reactive gas, e.g., N_2 or O_2, the sputter process becomes reactive. Unbalanced magnetrons of type II (see. Figure 2.5) are normally used for the deposition of these types of films and this configuration signifies stronger outer poles with respect to the center pole.

This leads to an enhanced ionization further away from the target and electrons from the target are allowed to move closer to the substrate increasing the ion flux at the substrate. Further details about sputtering and glow discharges can be found elsewhere [25,26].

To grow films consisting of more than two elements, one solution is to sputter from a compound target in a reactive gas. Another possibility is to use two sources and co-sputter in a reactive gas. The latter has the advantage of giving the possibilities of varying the composition of the films in a wider range (as was done in Paper I), as well as increasing the deposition rate. This work shows that ternaries can be grown by simultaneous sputtering of two targets in a nitrogen/argon mixed atmosphere.

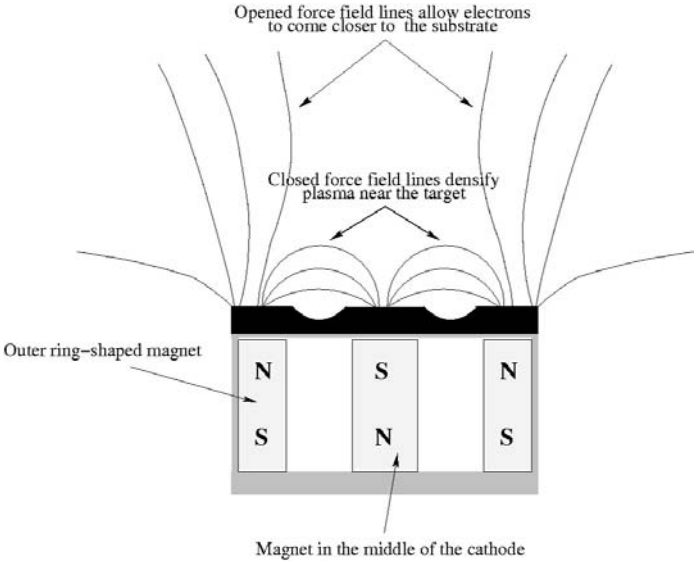

Figure 2.5: Schematics of an unbalanced magnetron with stronger outer magnets. (From Ref. [27]).

In Figure 2.6 an ultra high vacuum (UHV) deposition system used for co-sputtering of Si-C-N films is schematically presented. The Si-C-N films were grown with the magnetrons in an unbalanced mode, but with the plasma not coupled. This configuration was used in order to extend the plasma towards the substrate and to some extent avoid mixing of the sputtered yields from the sources. In conjunction

with a non-rotating substrate, the achievement of a compositional gradient on the substrate was possible.

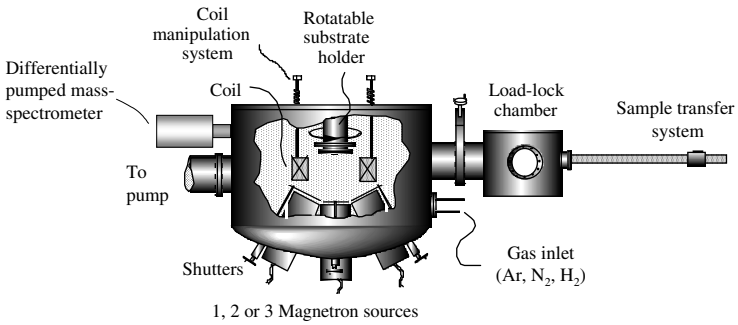

Figure 2.6: Schematics of the UHV deposition system used for growth of a-C, CN_x and SiCN films.

The SiCN and CN_x-films were sputtered in an ultra high vacuum system at a base pressure of $1x10^{-7}$ Pa and an Ar/N_2 discharge of 0.4 Pa (3mTorr). Both magnetrons were operated in a constant-current mode with a discharge current of 0.05 and 0.2 A for the Si and C targets, respectively. The BCN-films were sputtered in a high vacuum system at a base pressure of 1.33×10^{-5} Pa and the same Ar/N_2 discharge as for the previous mentioned films, and the magnetrons were operated with target currents varying in the range 0.1–0.4 A between different depositions.

2.5 Characterization of carbon nitride

2.5.1 X-ray Photoelectron Spectroscopy (XPS)

XPS is a surface sensitive analysis technique used for the analysis of elemental composition and the electronic state of surface atoms. When X-ray photons with a certain kinetic energy (E_k) are impinged onto a sample surface photoelectrons are emitted. The electrons are subsequently separated according to their kinetic energy and counted. The energy of the photoelectrons is related to the atomic and molecular environment from which they originated. Conservation of energy is required in the photoionization process and can be stated as

$$E_i + \hbar\upsilon = E_f + E_k \qquad (4.1)$$

where E_i is the initial state energy of the system, $\hbar\upsilon$ is the photon energy, E_f is the final state energy of the ionized system and E_k is the kinetic energy of the emitted photoelectron. With the initial and final state configurations the binding energy, E_b, of the photoelectron can be expressed as

$$E_b = E_f - E_i \qquad (4.2)$$

If the photon energy is well defined the binding energy of the electron can be derived via the photoelectric equation [28,29]

$$E_b = \hbar\nu - E_k \qquad (4.3)$$

The binding energy is related to the Fermi level and by grounding both the sample and the spectrometer, the Fermi level of both systems are at the same energy level. The kinetic energy of the emitted photoelectron is measured with a spherical deflection analyzer. The photoelectron is either accelerated or retarded by an amount equal to the difference between the work function of the sample, Φ, and the work function of the spectrometer, Φ_{sp}. The kinetic energy of the photoelectron is, when it reaches the analyzer,

$$E_{kin} = E_{kin}^{i} - (\phi_{sp} - \phi) \qquad (4.4)$$

where E_{kin}^{i} is the initial kinetic energy. The kinetic energy of the photoelectron at the sample related to the binding energy (with reference to the Fermi level) is

$$E_{kin}^{i} = \hbar\nu - \phi - E_b \qquad (4.5)$$

Equations 4.4 and 4.5 give the relation between binding energy and measured kinetic energy of the photoelectron

$$E_{kin} = \hbar\nu - E_b - \phi_{sp} \qquad (4.6)$$

Any change in the electronic state of the material generates a change in the binding energy, which is usually called the chemical shift. The binding energy is specific to each element and when an atom engages another atom making a bond, the binding energy is changed which can be seen as a shift in energy in the scan for intensity versus binding energy. Each chemical bond causes a characteristic peak shift and by comparing the peak position of a known standard the bond type can be identified.

Some problems are connected with the use of XPS for characterization of carbon nitrides. One problem is overlapping (and broad) peaks in both N1s and C1s core level spectra, leading to the consequence of difficulties in the interpretation of data

resulting in different assignments of the peaks in the literature [30]. Another problem is that the sample might undergo structural changes during the high energetic ion bombardment (sputter cleaning) that is frequently used prior to analysis. Nevertheless, the technique is still extensively used for characterization of CN_x films and can specifically be used for fingerprinting of the FL microstructure [31,32].

2.5.2 High Resolution Transmission Electron Microscopy (HRTEM)

Transmission electron microscopy (TEM) is a versatile analysis technique for determining the microstructure of a CN_x-film. Together with the selected area electron diffraction (SAED) method, where crystal structures and lattice parameters can be determined, it was used to verify the FL microstructure of the CN_x-films and ternaries in this work. Since all films studied were non-crystalline, the SAED patterns were only used for the determination of lattice-spacings of the microstructure.

The contrast mechanisms in TEM arise from elastic and inelastic collisions of electrons, resulting in transmitted and scattered beams. In conventional imaging, an aperture in the back focal plane allows only one electron beam to contribute to the image. If this beam is directly transmitted, a bright field (BF) image is obtained, whereas a dark field (DF) image is formed when the aperture is positioned to select a strong diffracted beam. In HRTEM, which can be used for studying film structures with an atomic resolution, the image is resulting from interference from more than one diffracted beam. At certain conditions regarding operation of the microscope, an image with the atomic planes viewed dark, and the spaces between the planes viewed bright, can be obtained. Examples of resolved atomic planes are observed in the fullerene-like CN_x and BCN films in Figure 2.7 (a) and (b).

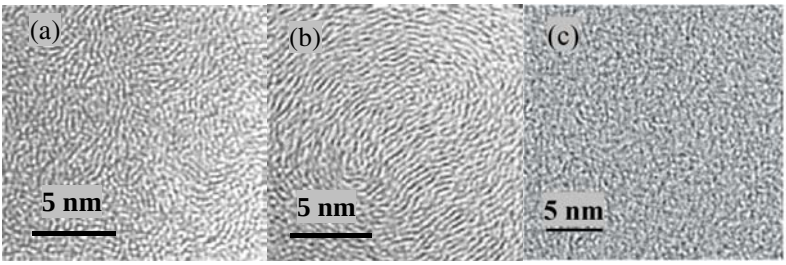

Figure 2.7: HRTEM plan-view images of (a) a fullerene-like CN_x film, (b) a fullerene-like BCN film and (c) an amorphous carbon film. In the fullerene-like structures ((a) and (b)), curved graphite-like basal planes, in average separated 0.35 nm, are resolved.

The sample preparation for HRTEM can either be fast and simple or very time-consuming and intricate. Plan-view samples can be prepared by lifting off very thin films (~20-50 nm) deposited onto NaCl substrates, by the dissolution of the substrate in de-ionized water. The thin films can then be collected on a microscope Cu-grid. A more intricate technique is ion etching of the samples to electron transparency after mechanical thinning to ~50 μm thickness. A disadvantage of the sample preparation by ion milling, besides the large preparation time already mentioned, is the risk of phase transformations appearing due to the exposure to the high-energy ion beam. For instance, amorphization or recrystallization may occur.

2.5.3 Atomic Force Microscopy (AFM)

Scanning probe microscopy (SPM) is one of the youngest surface characterization methods first demonstrated in 1981 by Binnig and Rohrer [33]. AFM, being one of several SPM techniques, is an analytical tool for obtaining information on the surface morphology and surface forces of a material. AFM can be used in a variation of set-ups, for surface potential measurements, electrical measurements or linked with nano-indentation to give a few examples. However, in this work AFM has only been used for topographical purposes. The principle of AFM is very simple. A sharp tip made of Si or Si_3N_4, mounted on an elastic cantilever is oscillated at a known frequency and scanned over the surface area while the surface forces between the tip and the sample

are recorded. The force is not measured directly, but calculated by measuring the deflection of the lever, and knowing the stiffness of the cantilever. The deflection of the cantilever is detected with a laser beam and a photodiode. In *contact mode* operation the interaction force between tip and sample is kept constant by adjusting the height over the surface. This is done by a real-time feedback of the detector's error signal to the piezoelectric scanner. In *tapping mode*, the cantilever is oscillated at a known frequency (close to its resonance) and the tip is in contact with the sample surface only a small fraction of its oscillation period. The tip height over the sample surface is constant and the interaction of the tip with the sample is modulating the cantilever oscillation. The cantilever oscillation amplitude is in this case steering the feedback responses. In both static and dynamic cases, the topography image is calculated based on the feedback response, which simply gives the surface tracked by the piezoelectric scanner while keeping the feedback parameter constant.

The simplicity of using this technique also makes it an excellent tool for evaluating surface roughness. The roughness is often quantified as a root-mean-squared (RMS) value and defined as,

$$\sqrt{\frac{1}{N}\sum (z_i - z_a)^2} \qquad (4.7)$$

where z_i are the z-values of all points, z_a the average z-value and N the number of points in the measured area, usually 1x1 μm^2. Another quantification of the surface roughness is the average roughness R_a, graphically defined as the area between the roughness profile and the center line divided by its evaluation length or, as the integral of the absolute value of the roughness profile height over the evaluation length.

2.5.4 Scanning Electron Microscopy (SEM)

The scanning electron microscope (SEM) is a versatile instrument that can be used for a variety of materials and analyses. Information about morphology, topography, elemental composition, crystal orientation, etc. can be obtained with different detection techniques, used in conjunction with the scanned electron beam. Even the analysis of conventionally "difficult" materials like insulators, semiconductors, low-density materials and low contrast materials can today be analyzed without major problems. With the second generation of instruments using

field emission for the creation of an electron beam, it is possible to analyze most of the above-mentioned materials by using lower accelerating voltages. This is possible thanks to lower energy spread within the beam and higher brightness of the source, which both minimize the chromatic aberration and hence improve the resolution of the microscope. An improved topographic contrast of small features, higher resolution and a decrease of charging are the most evident advantages for instruments equipped with field emission guns (FEG) operated at lower accelerating voltages.

The instrument used in this work was a Leo 1550 Gemini, equipped with a field emission gun. An internal secondary electron detector (in-lens) of the Leo 1550 SEM microscope, built into the column, gives "true" surface information of the sample by detecting only those electrons having the lowest energy, i.e. secondary electrons only generated directly by the electron beam. With the in-lens detector and operation at low accelerating voltage, it is possible to analyze the low-contrast materials CN_x, B-C-N and Si-C-N. Plan-views and cross-sections of these films can give information of the film growth, density and surface roughness, which vary from homogeneous, dense and smooth samples, to samples with textured structures and very rough surfaces. In Figure 2.8(a) a SiC-film grown at 700°C, with textured film growth and a faceted surface is shown. An example of a dense and smooth SiCN-film exhibiting low contrast is shown in Figure 2.8(b), whereas a g-CN_x film from Paper III and IV is shown in (c).

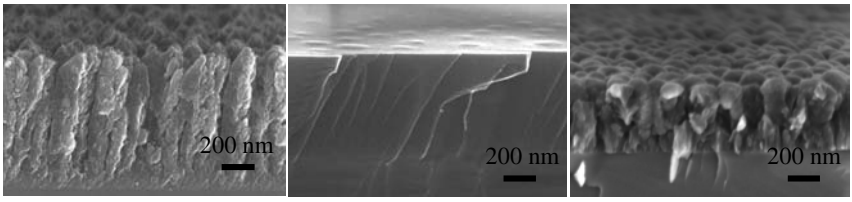

Figure 2.8: Cross-sectional secondary electron images of (a) a SiC film grown at 700°C and 100% Ar, (b) a SiCN film grown at 350°C and 15 % N_2 and (c) a g-CN_x film grown at 450°C and 100% N_2. All images were taken with in-lens detector at an acceleration voltage of 5 kV ((a) and (b)), or 2 kV (in (c)) at a working distance of ~4 mm.

The N-free Si-C films and the Si-C-N films with low concentrations of Si exhibited in general a surface with a more pronounced topography (as the example in

(a)). The surface roughness of the Si-containing films varied to a rather high extent whereas B-containing films and amorphous C and CN_x films overall showed smoother surfaces. The nanostructured g-CN_x and FL-CN_x films (in Paper III-IV) exhibited a more pronounced surface morphology compared to amorphous films.

2.5.5 Nanoindentation

The strength of a material depends on its resistance to deformation, which usually involves the movement of defects such as dislocations and/or formation of micro-cracks. There are several techniques applicable for testing of the mechanical properties of a material. Commonly used instruments for hardness measurements in industry are the Vickers and Rockwell indenters, so-called microhardness-testers. These instruments are not suitable for coatings in the micrometer or nanometer scale, since the indents are too large, so the result is mainly influenced by the substrate properties. A more suitable tool for thin films, from which hardness, elastic modulus as well as adhesion can be determined, is nanoindentation, which has been used in this work.

In nanoindentation, a diamond tip is indented into the sample surface, while the displacement, d, as a function of load, P, continuously is recorded. In Figure 2.9(a), a typical load-displacement curve from a nanoindentation experiment is shown, with the most important parameters that can be extracted from the curve presented. By analyzing the shape of the unloading curve, properties like hardness, H, and elastic modulus, E, can be extracted by different methods [34,35]. The most commonly used approach is to fit the upper part of the unloading curve to a power-law relationship ($P \propto (d\text{-}d_{res})^m$, where d_{res} is the residual displacement after load removal and m is a constant), which was suggested by Oliver and Pharr [35]. The upper part of the unloading curve is defined as the initial unloading stiffness, S, and together with an experimentally derived tip area function, hardness and modulus can be calculated. This method works well for plastic materials with well defined unloading behavior. For elastic materials, like some films in this work (see Figure 2.9(b)) for a typical elastic behavior), the exponent m is not constant during unloading, meaning that the contact area is not well defined during unloading. The true contact area is then normally overestimated, leading to an underestimation of the hardness values.

Another method, more suitable for elastic material, is developed by Hainsworth *et al.* [36] and suggests the analysis of the loading curve instead of the unloading curve.

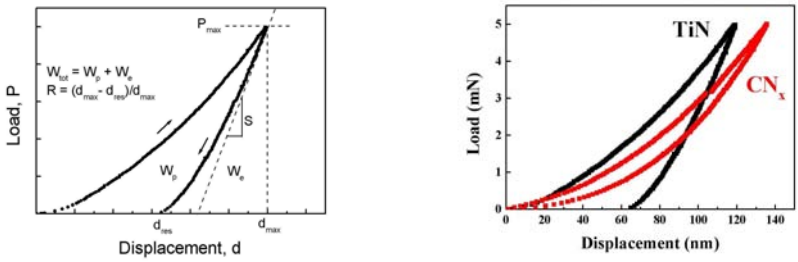

Figure 2.9: (a) A typical load-displacement curve from a nanoindentation experiment displaying the parameters that can be extracted from the curve. Indentation load (P_{max}); maximum displacement (d_{max}); residual displacement (d_{res}); S (initial unloading stiffness); elastic and plastic work of indentation, meaning the work used for deforming the material plastically and elastically during the indent (W_e and W_p); and finally, the elastic recovery (R). (From Ref. [35]) (b) Typical load-displacement curves from a nanoindentation experiment of TiN and CN_x film. The latter curve indicates a highly elastic behavior, characteristic for fullerene-like CN_x.

Although the evaluation of nanoindentation experiments on elastic materials is not easily performed, the load-displacement curve itself can be used as a "nanomechanical fingerprint" of the material. Instead of presenting hardness and modulus values, maximum displacement, d_{max}, at a specific load and the elastic recovery, R, defined as $R = (d_{max} - d_{res}) / d_{max}$, are characteristic values that can be extracted from the load-displacement curve. These values can readily be compared for different materials. This approach has been used for the films analyzed in Paper II, whereas hardness values were calculated in Paper I.

2.5.6 Contact angles and wetting

In addition to the requirements for a coating in engineering applications (e.g. hardness, low friction, and wear resistance) there are certain applications where also the *surface energy* is of concern. This surface property affects the *wettability* with

respect to water or oils (lubricants), or the cladding of material in contact with the coated part. These properties are not commonly investigated nor presented in literature so far and some confusion can be noticed. Some of the confusion lies in the definition of surface free energy and its close relation to the wettability of surfaces, which easily can be described by *contact angle* measurements.

The definition of surface free energy, γ, is half the energy needed to separate two flat surfaces from contact to infinity, having the unit energy per unit area; J m^{-2}. For liquids, γ is commonly denoted γ_L and is usually given in units of tension per unit length; N m^{-1}, which is numerically and dimensionally the same as the surface free energy [37]. Surface tension can also be defined as a force that operates on a surface and acting perpendicularly and inward from the boundaries of the surface, tending to decrease the area of the interface. Wettability is not a physical property, but very often used as a description of how well a liquid will spread over a surface and thereby giving information about the surface energy of the material. Other words to describe the wettability of a surface, and more often used in biotechnology, is hydrophobic and hydrophilic surfaces.

There are several methods used for determination of the surface free energy of solids and liquids. Some are very simple and have been used in the same manner for several decades, e.g., a variety of methods for contact angle measurements giving information of the wettability of a material. It can also be used for calculation of the surface free energy. There are also newer, more sophisticated instruments useful to measure surface energies directly. For example a modified Atomic Force Microscope can be used to measure the forces between two solids or a solid and a liquid. A sphere of the material to be analyzed is glued onto a cantilever and the repelling or attracting forces between the sphere and a liquid or another solid can be measured [37].

In this work the so-called sessile-drop method has been used. It can be used for calculation of the surface free energy of the surface, but often the information given only from the contact angle values are a satisfactory result as it is an estimate of the wettability of the material.

Contact angle measurements as a means to characterize surfaces have been practiced for a long time, and the famous Young's equation presented below dates back to the early nineteenth century [38]. The sessile-drop technique used in this work is a rather simple method and the set-up consists of a surface, a gas and a liquid as

illustrated in Figure 2.10. A droplet of the liquid is carefully placed on the solid of interest and adopts a shape that minimizes the total free energy of the system.

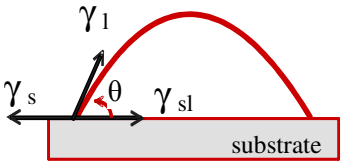

Figure 2.10: Principle of the sessile-drop method, where a droplet of a liquid is placed on the surface of the solid to be examined. The figure shows a case where the liquid do not spread out on the surface, giving a large contact angle, θ, which can be attributed to materials with low surface energy.

A characteristic contact angle, θ, appears, depending on the interface tension between the solid, liquid and gas in the point of contact. The contact angle is measured using an optical contact angle meter and the value is either simply compared with other materials, or used for calculation of the surface free energy. Droplets, ~3 mm in diameter, are carefully placed onto the surface and with the tip of the syringe still in touch with the droplet it is possible to measure two contact angle values, one advancing (θ_a) and one receding angle (θ_r). The advancing angle is measured when the amount of liquid in the droplet is increasing, whereas the receding angle is measured when the amount of liquid in the droplet decreases. These two angles yield information about the important parameter, $\Delta\theta=\theta_a-\theta_r$, called the contact angle hysteresis. This provides information about the heterogeneity of the surface. Generalized, the larger the value of Δθ, the more heterogeneous the surface is. Heterogeneities are generally attributed to surface roughness, chemical heterogeneity, or both. If the measurements are performed with at least two different solvents the contact angles can be used for calculation of the surface free energy as follows. The equilibrium state between the solid, liquid and gas in the point of contact can be described by a simplified Young's equation [38]:

$$\gamma_s = \gamma_{sl} + \gamma_l \cos\theta, \qquad (4.8)$$

where γ_s, γsl and γl is the surface free energy of the solid, the interface between solid and liquid, and liquid, respectively.

2.5.7 Ellipsometry

In Paper III the optical properties of the carbon-based films were determined and analyzed in the UV-Vis-NIR and IR spectral ranges using spectroscopic ellipsometry (SE) for further information about the microstructure and for comparison with results from HREM and XPS. In this technique polarized light is used to determine the change of polarization state due to reflection at a sample surface. The change in polarization state is described by the ellipsometric angles Ψ and Δ, which are the relative amplitude-change and the phase change, respectively, of p- and s-components of the incident wave. The p- and s- coordinates are defined relative to the plane of incidence, where p stands for parallel and s (senkrecht) stands for perpendicular. By fitting a complex-valued model dielectric function $\varepsilon = \varepsilon_1 + i\varepsilon_2$ to experimental Ψ and Δ data, optical resonances can be determined and correlated to certain bonds in the carbon and CN_x films.

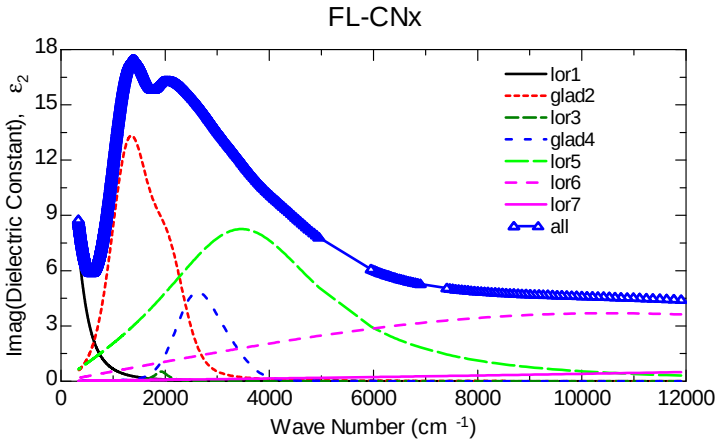

Figure 2.11: Ellipsometric spectra of the FL-CN_x film showing the imaginary part of the dielectric function modeled with Lorentz and GLAD oscillators.

An optical model with Lorentz oscillators was used for analyzes of the carbon and CN_x-films in Paper III. The films showed a rich variety of absorption bands related to the materials local bonding structure. The spectrum from one of the films with seven resonances fitted to experimental data is shown in Figure 2.11. Five of these resonances could be related to a specific bonding structure identified by other authors

measured with SE or fourier transform infrared spectroscopy. Spectroscopic ellipsometry will be described in more detail in chapter 4.

2.6 Carbon-based materials in medicine

There is an increased demand for novel coatings or surface modifications in biotechnological areas, e.g. biofouling, improvements of the bonding between bone and implant, increased demands in food processing industries as well as coatings and surfaces on medical devices and better biocompatibility of sensors. Here, only medical applications of carbon-based materials will be considered.

2.6.1 Carbon and carbon nitride as biomaterials

Carbon-based materials (commonly in the form of DLHC and pyrolytic carbon) are today frequently used as replacement for certain parts of the body and in numerous of medical devices, e.g. artificial heart valves, vascular stents, load-bearing joints and catheters drainage tubes and polymer contact lenses. Most of the applications require blood compatible materials. The use of amorphous carbon and DLHC in medical applications is not as anchored as is the use of pyrolytic carbon, nevertheless its potential as a biomaterial is promising. Studies on blood compatibility of DLHC has been ongoing for at least a decade [39,40], whereas the oldest studies on the blood compatibility of a-C are a few years old [41] and show promising results.

Amorphous carbon films have been tested for cytotoxicity using several cell lines, e.g., Rodil et al. used osteoblast cells for the test of changes in cellular response (e.g. cell death, altered cellular morphology and inhibition of biosynthetic functions) with results showing no toxic effects from a-C surfaces [42].

In addition, Rodil et al. have reported results of osteoblast and fibroblast attachments onto sputtered carbon and carbon nitride thin films showing non-toxicity and similar biocompatibility compared to conventional orthopedic/dental implants [43]. Only a few experiments have been reported regarding the haemo-compatibility of CN_x [44-46] but initial studies by Maitz et al. showed promising results of protein adsorption as well as platelet adherence on BCN films [48].

The ability of CN_x surfaces to induce biomineralization has so far only been studied to a limited extent [49].

References

[1] D. C. Elias, R. R. Nair, T. M. G. Mohiuddin, S. V. Morozov, P. Blake, M. P. Halsall, A. C. Ferrari D. W. Boukhvalov, M. I. Katsnelson, A. K. Geim, K. S. Novoselov, Science 323 (2009) 610-613.

[2] A.Y. Liu, M.L. Cohen, Science 245 (1989) 841-842.

[3] A.Y. Liu, M.L. Cohen, Phys. Rev. B 41 (1990) 10727-10734.

[4] H. Sjöström, S. Stafström, M. Boman, J.-E. Sundgren, Phys. Rev. Lett. 75 (1995) 1336-1339.

[5] M. Kohzaki, A. Matsumuro, T. Hayashi, M. Muramatsu, K. Yamaguchi, Thin Solid Films 239 (1997) 308-309.

[6] R. Gago, I. Jiménez, D. Cáceres, F. Agulló-Rueda, T. Sajavaara, J.M. Albella, A. Climent-Font, I. Vergara, J. Räisänen, E. Rauhala, Chem. Mater. 13 (2001) 129-135.

[7] J.-P. Palmquist, S. Li, P.O.Å. Persson, J. Emmerlich, O. Wilhelmsson, H. Högberg, M.I. Katsnelson, B. Johansson, R. Ahuja, O. Eriksson, L. Hultman, U. Jansson, Phys. Rev. B 70 (2004) 165401.

[8] T. Thärigen, G. Lippold, V. Riede, M. Lorenz, K.J. Koivusaari, D. Lorenz, S. Mosch, P. Grau, R. Hesse, P. Streubel, R. Szargan, Thin Solid Films 348 (1999) 103-113.

[9] A. Bendeddouche, R. Berjoan, E. Bêche, T. Merle-Mejean, S. Schamm, V. Serin, G. Taillades, A. Pradel, R. Hillel, J. Appl. Phys. 81 (1997) 6147-6154.

[10] E. C. Samano, R. Machorro, G. Soto, L. Cota-Araiza, J. Appl. Phys. 84 (1998) 5296-5305.

[11] P. Jedrzejowski, J. Cizek, A. Amassian, J. E. Klemberg-Sapieha, J. Vlcek and L. Martinu, Thin Solid Films 447-448 (2004) 201–207.

[12] A. Badzian, T. Badzian, R. Roy, W. Drawl, Thin Solid Films 354 (1999) 148-153.

[13] W.F.A Besling, A. Goossens, B. Meester, J. Schoonman, J. Appl. Phys. 83 (1998) 544-553.

[14] M. Grischke, K. Bewilogua, K. Trojan, H. Dimigen, Surf. Coat. Technol. 74-75 (1995) 739-745.

[15] R. Riedel, Adv. Mater. 6 (1994) 549-560.

[16] L. Filipozzi, A. Derré, J. Conard, L. Piraux, A. Marchand, Carbon 33 (1995)

1747-1757.

[17] R. Gago, I. Jiménez, I. García, J.M. Albella, Vacuum 64 (2002) 199–204.

[18] D. Hegemann, R. Riedel, and C. Oehr, Thin Solid Films 339 (1999) 154-159.

[19] N. Hellgren, *"Sputtered Carbon Nitride Thin Films"*, Doctoral Thesis No. 604, Linköping University, Linköping, Sweden, 1999.

[20] H. Sjöström,*"Thin Films of Amorphous Carbon and Carbon Nitride",* Doctoral Thesis No. 401, Linköping University, Linköping, Sweden, 1995.

[21] G.K. Gueorguiev, J. Neidhardt, S. Stafström, L. Hultman, Chem. Phys. Lett. 410 (2005) 228-234.

[22] W.J. Gammon, Doctoral Thesis, College of William and Mary, Williamsburg, Virginia, USA, 2003.

[23] H.W. Kroto, J. R. Heath, S. C. O'Brien, R. F. Curl, R. E. Smalley, Nature 318 (1985) 162-163.

[24] G. Fanchini, A. Tagliaferro, "Correlation between local structure and film properties in amorphous carbon materials", G. Messina, S. Santangelo (Eds.), Carbon, topics in Applied Physics, Springer-Verlag, Berlin, 2006.

[25] B.N. Chapman, Glow Discharge Processes, Wiley and Sons, New York, 1980.

[26] B. Window, N. Savvides, J. Vac. Sci. Technol. A4 (1986) 453-456.

[27] A. Furlan, *"Fullerene-like CN_x and CP_x thin films; synthesis, modeling and applications",* Doctoral Thesis No. 1247, Linköping University, Linköping, Sweden, 2009.

[28] A. Einstein, Ann. Phys. 17 (1905) 132-148.

[29] H. Luth, Solid Surfaces, Interfaces and Thin Films, 4th edn., Springer, Germany, 2001.

[30] S.E. Rodil, S. Muhl, Diamond Rel. Mater. 13 (2004) 1521-1531.

[31] N. Hellgren, M.P. Johansson, E. Broitman, L. Hultman, J.-E. Sundgren, Phys. Rev. B 59 (1999) 5162-5169.

[32] J. Neidhardt, L. Hultman, Zs. Czigány, Carbon 42 (2004) 2729-2734.

[33] G. Binnig, H. Rohrer, Ch. Gerber, E. Weibel, Appl. Phys. Lett. 40 (1982) 178-180.

[34] M.F. Doerner, W.D. Nix, J. Mater. Res. 1 (1986) 601-609.

[35] W.C. Oliver, G.M. Pharr, J. Mater. Res. 7 (1992) 1564-1583.

[36] S.V. Hainsworth, H.W. Chandler, T.F. Page, J. Mater. Res. 11 (1996) 1987-1995.

[37] J. Israelachvili, Intermolecular & Surface Forces, 2:nd ed., 1991.

[38] T. Young, Phil. Trans. R. Soc. 95 (1805) 65-87.

[39] F.Z. Cui, D.J. Li, Surf. Coat. Technol. 131 (2000) 481-487.

[40] R. Hauert, Diamond Relat. Mater. 12 (2003) 583-589.

[41] S. Logothetidis, M. Gioti, S. Lousinian, S. Fotiadou, Thin Solid Films 482 (2005) 126-132.

[42] S.E. Rodil, "Biocompatibility, cytotoxicity and bioactivity", G. Messina, S. Santangelo (Eds.), Carbon, Topics in Applied Physics, Springer-Verlag, Berlin, 2006.

[43] S.E. Rodil, R.Olivares, H.Arzate, S.Muhl, Diamond Rel. Mater. 12 (2003) 931–937.

[44] C.L. Zheng, F.Z. Cui, B. Meng, J. Ge, D.P. Liu, I.-S. Lee, Surf. Coat. Technol. 193 (2005) 361-365.

[45] Z.R. Wu, M. Zhang, F.Z. Cui, Surf. Coat. Technol. 201 (2007) 5710-5715.

[46] F.Z. Cui, X.L. Qing, D.J. Li, J. Zhao, Surf. Coat. Technol. 200 (2005) 1009-1013.

[47] F.Z. Cui, D.J. Li, Surf. Coat. Technol. 131 (2000) 481-487.

[48] M.F. Maitz, R. Gago, B. Abendroth , M. Camero , I. Caretti , U. Kreissig, J. Biomedical Res. Part B: Applied Biomaterials 77 (2005) 179-187.

[49] R. Olivares, S.E. Rodil Surf. Coat. Technol. 177-178 (2004) 758-764.

Chapter 3
Macromolecular interactions

Macromolecular interactions are of outmost importance in a wide range of disciplines, e.g. medicine, biomaterial technology, biotechnology, nanotechnology, and sensor technology, areas that have been subject for increased interest during the last decades and show rapid development. The word macro-molecule derives from the Greek word macro - meaning "long" or "large", and the Latin word moles - meaning "small unit of mass" [1,2]. In the context of biochemistry, the term may be applied to nucleic acids, proteins, carbohydrates and lipids. Conventionally, macromolecules are considered to involve proteins and artificial polymer chains as well as naturally occurring polymers. In this work proteins were used, and more particularly, experiments were made with single protein solutions and blood plasma. It is, however, important to keep in mind that in order to obtain a proper assessment of e.g. an implant in contact with the human body, other tests have to be performed as well. For example cell-, animal- and complex protein solution experiments have to be performed to reveal the impact of activation complement (the immune system) and coagulation. Finally an in vivo study with human patients has to be performed in order to follow the healing process in which proteins, cells and organs, i.e. the entire host system, is involved. However, protein adsorption tests can be used as a first indication on how a surface will interact with body fluids.

3.1 Biomaterial

3.1.1 What is biocompatibility and bioactivity?

The traditional definition of a *biomaterial* is …"any substance (other than drug) or combination of substance, synthetic or natural in origin, which can be used for any period of time, as a whole or as a part of a system which treats, augments or replaces any tissue, organ or function of the body"…[3]. Modern biomaterial science includes also materials used in biosensing and bioelectronic applications, as well as materials used for implantation and drug delivery. There are other definitions and often more general descriptions of a biomaterial, e.g. ..."substances other than food or drugs contained in therapeutic or diagnostic systems that are in contact with tissue or biological fluids" [4]. In addition, there are several different classifications of biomaterials, e.g. there is a difference between biological materials (made from biological materials) and (often artificial) materials for biological interactions.

Biocompatibility is a technical term that sometimes is used a bit careless in biomaterial science. Several definitions have been expressed during the years, e.g. "a material that is not harmful or toxic to living tissue" [5] or "a synthetic material which has been formulated to be used in humans without causing any harm or immunological response".

Bioactivity is another term that may need some explanation. A material is considered bioactive if it has positive interaction with, or effect on, any cell tissue in the human body. In biomineralization studies, bioactivity means the ability of a surface to induce the formation of calcium phosphate (CaP, $Ca_5(PO_4)_3(F,Cl,OH)$) crystals at surfaces in a simulated body fluid, a buffer solution with ion contents similar to that of human blood.

3.1.2 Problems regarding biomaterials and biotests

A large number of medical devices are implanted in the human bodies every year, both regarding types and numbers. Hip joints, orthopedic screws and pins, heart valves, stents, dental roots and ocular lenses are a few examples. However, very few surfaces are truly biocompatible. Problems exist, with corrosion in body fluids, generation of wear particles in articulating systems, infections and blood coagulation and cellular damage leading to impaired functionality and ultimately to implant

failure. Thus, there is still a need to improve biomaterials [6,7]. For example titanium, known to be compatible with the human body, is found to be thrombogenic [8,9], meaning that coagulation (thrombus formation) occurs upon contact with blood.

The process of following a material from "birth" to a final commercialization is generally very long and the material must pass a series of tests in terms of its biocompatibility and toxicity. Depending on the use of the material, different tests are performed to determine its hemolytic, toxic, immunologic and thrombotic properties. To generalize, the testings start with dissolution tests in buffers, followed by adsorption analysis in single protein solutions or human blood plasma. The evaluation continues with studies in *in vitro* cell cultures of e.g. osteoblasts, fibroblasts, or leukocytes. Later in the process, numerous of *in vivo* animal tests are performed. The meaning of *in vitro* is that biological processes are performed in a controlled environment outside the living organism, e.g. in a laboratory vessel. A problem that follows is the uncertainty regarding the correlation between *in vitro* and *in vivo* experiments.

In the present work, *in vitro* adsorption tests in single protein solutions and human blood plasma were implemented. Surface-located and accessible proteins after blood plasma incubations were eventually identified through incubations in antibody solutions.

3.2 Proteins at interfaces

Proteins are macromolecules playing an important role in virtually all kinds of biological interactions. They catalyze reactions, regulate cells and chemical processes in the human body in the form of enzymes, hormones, antibodies and balance body water and nutrition. Proteins are involved in processes like coagulation, cellular and humoral immunological processes, transport, inflammation and wound healing. When biomaterials are implanted into animals or humans, protein adsorption to foreign surfaces occur within milliseconds of contact [10]. The rapid adsorption leads to that cells arriving at the biomaterial surface probably interact with the adsorbed protein layer rather than directly with the material itself. Thus, the initial protein adsorption onto a biomaterial surface plays a key role in body responses toward a foreign implanted biomaterial. This is further discussed in chapter 3.4.

Proteins differ not only in function but also in structure and molecular mass. In human and animal bodies the number of different proteins reaches up to 30 000, ranging in size from a few kDa (1 Da is very close to the weight of one H atom) to more than a thousand kDa. Proteins are not only large but also very complex polypeptides consisting of a sequence of amino acids linked together with peptide bonds. The amino acid sequence is determined by the genetic code stored in cell DNA and is called the primary structure of the protein. The protein secondary structure is α-helices, β-sheets and β-turns stabilized by hydrogen bonds, and the tertiary structure is the three-dimensional folding of the polypeptide chain with the hydrophobic effect and internal dehydration of surfaces as the main driving force. This leads to non-polar amino acid side chains preferentially becoming buried inside the core of the protein while polar chains become exposed on the outer domains of the protein. The quaternary protein structure describes the arrangement and position of each of the subunits in a multiunit protein (See any book in biochemistry e.g. [11]).

Depending on the nature of the amino acid side-chain, the amino acid can be hydrophilic (water-attracting) or hydrophobic (water-repelling), acidic or basic in character; and it is this diversity in side-chain properties that finally gives each protein its specific character. Proteins are amphiphilic meaning they possess both hydrophobic and hydrophilic groups, and this makes them surface active. Protein adsorption to surfaces can either be beneficial or a problem, depending on the area of practical use of the material. Sometimes adsorption is desired, as in food additives, to stabilize food emulsions (for prolonged shelf life) or in artificial bone replacements, and sometimes not, like on blood contacting artificial material (e.g. heart valves) or in biotechnological processes.

In haemocompatibility studies the ratio of adsorbed amount of albumin to fibrinogen is often measured. The albumin/fibrinogen ratio is a measure of platelet adhesion and activation, where a high ratio indicates a less thrombogenic material [12].

3.3 Proteins used in the present work

3.3.1 Fibrinogen

Fibrinogen (Fib) is a fibrous but soft [13] and soluble glycoprotein synthesized in the liver and has a human blood plasma concentration of 1.5-4.0 g/L. The protein is involved in several important processes in the human body, such as haemostasis (blood coagulation and fibrinolysis (dissolving of blood clots)), wound healing, inflammation, angiogenesis, and cellular interactions. These processes involve the conversion of fibrinogen to fibrin, and often also the interaction of fibrin(ogen) with various proteins and cells. At injury Fib transforms to fibrin in presence of thrombin, and fibrin monomers link together to a cross-linked fibrin polymer (fibrin assembly) forming a fibrin clot. The process is regulated by interactive sites on fibrinogen, which evolve as fibrinogen is converted to fibrin, or through fibrinogen-surface interactions [14].

The trinodular shape of Fib was proposed from electron micrographs in 1959 by Hall and Slater [15]. They stated the overall length of the molecule to be 47.5±2.5 nm. Later, a Fib structure consisting of six peptide chains (two each of α, β, and γ) in two rod like regions has been established and today most authors suggest that the molecule is 45 nm in length (Figure 3.1). The polypeptides are oriented in such a way that all six N-terminal ends (the amino end of the peptide) meet in a central E domain. Two regions of coiled coil alpha helices stretch out on either side of the E domain, each consisting of one Aα, one Bβ and one γ polypeptide. The C-terminus (the carboxyl end of the peptide) of each chain folds independently in a separate globular D domain. The α-chain is longer than the two other, and its C-terminal folds back to form a single globular domain close to the central domain E. Depending on the conditions, the C-termini of α-chains and the E domain can either form disulphide bonds or be separated.

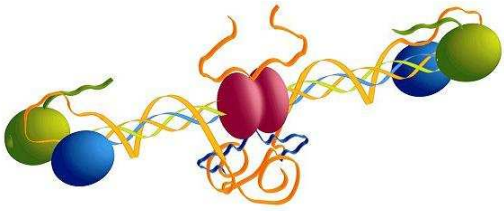

Figure 3.1 Schematic of human serum fibrinogen with the six peptide chains ending up in the E and D-domains. The central domain (red) is referred to as the E-domain and the green and blue domains are referred to as being D-domains. (see text for explanation)(http://www.pathology.unc.edu/faculty_labs/lord_lab/)

Both negatively and positively charged areas of the molecule are exposed, the D and E domains are negatively charged [16] whereas the αC domain is positive. The αC domain possesses both hydrophobic and hydrophilic regions and it therefore easily changes its conformation and has the possibility to electrostatically adhere to surfaces. The adhesion of the αC domain is not very strong, but is often claimed as the starting event during adsorption, followed by adhesion of D and E domains. Studies of the three-dimensional structure of the fibrinogen molecule have covered two thirds of the molecule, including the complete D regions and most of the E region, whereas the αC domains remain to be fully determined [17].

Fib was chosen as the model protein in Paper V due to its low immunoactivity (low complement deposition to adsorbed fibrinogen from plasma) and the possibility to incorporate drugs in a structure consisting of a Fib matrix. In addition, a large flexible protein facilitates the preparation of thick protein layers.

3.3.2 Human serum albumin

Human serum albumin (HSA) is a soft globular protein and can be found in human blood at a concentration of 35-55 g/L. The protein has numerous physiological functions, such as regulating the osmotic pressure in blood, and being a transporter of fatty acids and bilirubin. In addition, adsorbed albumin is generally considered to

"passivate" a surface and during shorter contact times (hours) largely reduce the acute inflammatory response to implanted materials [18,19].

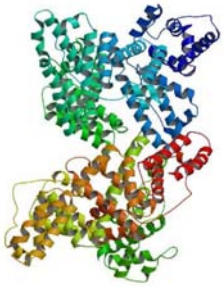

Figure 3.2 Schematic of human serum albumin obtained from the protein data bank. [http://www.rcsb.org, accessed 1 June, 2009]

Table I shows the isoelectric points of albumin and fibrinogen, and also their molecular sizes. Albumin was used as a model protein in Paper IV.

Table I: Properties of human fibrinogen and albumin

Protein	Isoelectric point	Molecular weight (kDa)	Molecular size (nm^3)	Reference
Fibrinogen	5.5	340	6x6x45	[20]
Albumin	5.16 (at 0.15 M)	66	3x3x8	[21]

3.4 Protein adsorption

Why study protein adsorption? Because biomolecule-surface interactions are crucial to biological systems and to a large numbers of industrial processes. The understanding of the fundamental factors that determine protein adsorption is necessary to improve our ability to design biocompatible materials and devices. Therefore, protein adsorption studies are commonly performed as tools for testing of general bioactivity. They have in fact become a standard testing procedure during initial stages in the development of new materials.

Several driving forces are known for protein adsorption, an exothermic process described by $\Delta G=\Delta H-T\Delta S$, where ΔG=change in Gibbs free energy, ΔH=change in enthalpy, T=temperature and ΔS= change in entropy. According to the literature, the major force is the dehydration of surfaces leading to a decrease in the systems Gibb's

free energy (ΔG) via increased system entropy (+ΔS). A surface also affects proteins conformational changes of proteins (for a so called soft protein) and by electrostatic attraction/repulsion (more important for a so called hard protein) [22]. Other important factors upon close protein/surface contact dispersion forces are surface energy and surface roughness. The properties of the solution, such as pH and salt concentration, also greatly affect the adsorption. In addition, mass transport of the solute to and from the surface, is essential for protein adsorption [23].

Until a few years ago it was a common belief that protein molecules were fully denatured upon adsorption. This has turned out not to be true, rather the protein molecule undergoes conformational changes to a larger or smaller extent upon adsorption to a solid surface. So called soft molecules or structurally labile molecules (like fibrinogen and albumin) undergo larger conformational changes compared to hard molecules or structurally stable molecules (like collagen and keratine). The conformational changes involve reduction of ordered structures leading to unfolding and increased internal mobility [22]. This in turn increases the system entropy. The folding and unfolding is hence related to the stability of a protein. A kinetically stable protein will unfold more slowly compared to a kinetically unstable protein.

Most proteins adsorb more readily to hydrophobic surfaces than to hydrophilic, due to that surface-bound water is less tightly bound to hydrophobic surfaces than to hydrophilic surfaces and the conformational changes in adsorbing proteins are more pronounced at hydrophobic surfaces [24,25]. Both effects contribute to a larger ΔS of the system.

3.4.1 Chemical surface activation and cross-linking

Sometimes an increased bonding strength between a protein and a surface is desired, e.g. when PEGs[1] are bound to surfaces to resist protein adsorption, when blood contacting materials are heparinized to reduce activation of coagulation or when thick protein matrices are aimed to be formed. A common procedure is to use linkers between the protein molecules and the surface. In Paper V silicon surfaces were activated by silanisation using 3-aminopropyl-trietoxysilane (APTES) $(H_2N(CH_2)_3Si(OC_2H_5)_3$ forming a linker with accessible -NH_2 groups on the surface. The silicon surfaces were then exposed to glutaraldehyde (GA), a cross-linker with

[1] Poly(ethylene glycol) is a polymer used in several biomedical applications.

reactive amine binding aldehyde groups in both ends and often used in biochemical applications, producing a functionalized surface with accessible -CHO groups (Figure 3.3).

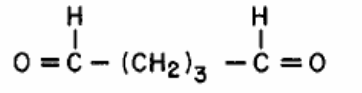

Figure 3.3 The glutaraldehyde molecule commonly used as a cross-linker.

A direct cross-linking method with the concept to activate carboxyl (-COOH) groups has also been used in Paper V. The concept is referred to as EDC/NHS affinity ligand coupling chemistry and is a well established procedure [26]. Activated carboxyl groups react easily with amine groups forming a peptide bond. One important difference with this method compared to the use of a cross-linker such as GA, is that no cross-linking agents are incorporated in the material.

3.4.2 Methods for monitoring protein adsorption

Several methods are used for protein adsorption studies, of which the most common are optical and spectroscopic techniques. Some of the methods will be briefly described below.

The most frequently used optical methods are the *surface plasmon resonance* (SPR) technique first presented in 1983 [27] and *ellipsometry* [24,28]. SPR is a technique which utilizes the phenomenon that occurs when light is internally reflected off a thin metal film on a glass prism. The incident light can at a certain angle interact with electrons in the metal film (plasmons), thus reducing the reflected light intensity. The angle where this resonance occurs is dependent of the refractive index of the metal and the ambient medium which is a liquid in the case of protein adsorption studies. The high sensitivity of the SPR angle to changes in near-surface refractive index of the liquid ambient can be used to detect biomolecules at the liquid-gold interface. SPR is a convenient method for studies of the kinetics of adsorption to surfaces, but requires the use of a noble metal surface.

Ellipsometry is based on the change of polarization of light due to reflection at a surface. This means that the surface properties of the sample influence the change of polarization of the light. The most common mode of ellipsometry used for the study

of protein adsorption is the nulling mode using a single wavelength light source. Since only one set of data points then is available the ellipsometric data are mainly sensitive to the optical mass *nd*, where *n* is the refractive index of the protein film and *d* its thickness. A value of *n* then normally is assumed and *d* can be determined. The thickness obtained in this way is then a fictitious parameter and its value depends on the index chosen. To avoid the problem with assuming a incorrect refractive index, spectroscopic ellipsometry may be used. In this case both *n* and *d* can be determined unambiguously. Ellipsometry is a non destructive method, where real time and *in situ* measurements are possible. It is a sensitive technique which is fairly simple to handle. One has to keep in mind though, that homogeneous optical parameters in the layers are assumed.

Optical waveguide lightmode spectroscopy (OWLS) is based on grating-assisted coupling of light into and guidance within an optical waveguide layer [29]. Transverse electric (TE) and transverse magnetic (TM) modes can be excited by varying the angle of incidence of the light beam. Disadvantages with the method are that only highly transparent surfaces can be investigated and that the film thickness can only be calculated provided that the refractive index of the protein film is known.

Reflectometry is another optical method where incident waves are reflected at an interface and the intensity and angle of the reflected waves are measured as a function of the incident angle and/or wavelength. The technique applies to any form of wave, however, it has become particularly popular for electromagnetic radiation. More recently, *neutron reflectometry* has emerged as a powerful and complementary technique to X-ray reflectometry. Neutron reflectometry gives information about molecular orientation of a protein layer.

The *quartz crystal microbalance technique* (QCM) is a method using changes in the resonant frequency of a quartz crystal to follow adsorption in the monolayer range. The frequency shift which is due to a change in the total adsorbed mass, which includes hydro-dynamically coupled water and water associated with the hydration layer of e.g. proteins and/or water trapped in cavities in the layer. This is an apparent complication of the method.

Differential scanning calorimetry (DSC), which is a tool for the investigation of the structural stability of a protein, combines traditional equilibrium calorimetry with dynamic analyses of thermal processes.

Infrared reflection-absorption spectroscopy (IRAS) uses infrared light at near-grazing incidence to a surface. The electric fields of incident and reflected light are separated into two components, parallel and perpendicular to the plane of incidence. This technique can provide information about the orientation of protein molecules. A drawback of the technique is the requirement of a highly reflecting substrate.

A last method to be mentioned is *Circular dichroism* (CD), which is an optical as well as spectroscopic method, and uses circularly polarized light to measure the secondary or tertiary structure of proteins in solution. Left- and right-circularly polarized light of equal amounts is radiated into a solution and either left- or right-circularly polarized light is absorbed more than the other and this wavelength dependent difference of absorption is measured [30]. This technique is restricted to be used at wavelengths where light absorption takes place and in addition the technique can not be used for monitoring of adsorption processes.

3.5 Complement activation and contact activation

To get somewhat reasonable information about the biocompatibility of a surface, or more correctly its concurrence with biomolecules, it is necessary to expose the surface to proteins which in turn may start the blood coagulation cascade and/or trigger the immune system in body fluids. The immune system is in principle comprised of a cellular part and a protein mediated part (so called humoral, and mainly mediated by antibodies) for the protection of our bodies. The proteins of the complement system participate in the combat against bacteria, viruses, fungi, cancer cells or other foreign materials, but may also be active on implants. The complement system consists of the immune system in blood. It consists of more than 30 different proteins and involves three activation pathways; the classical, the alternative and the lectin pathways, see Figure 3.5. Complement factor 3 (C3) is one of the key controlling points of all pathways. It is involved in the alternative pathway and the deposition of C3b (cleaved C3) at a surface can therefore be used as recognition for complement deposition or activation.

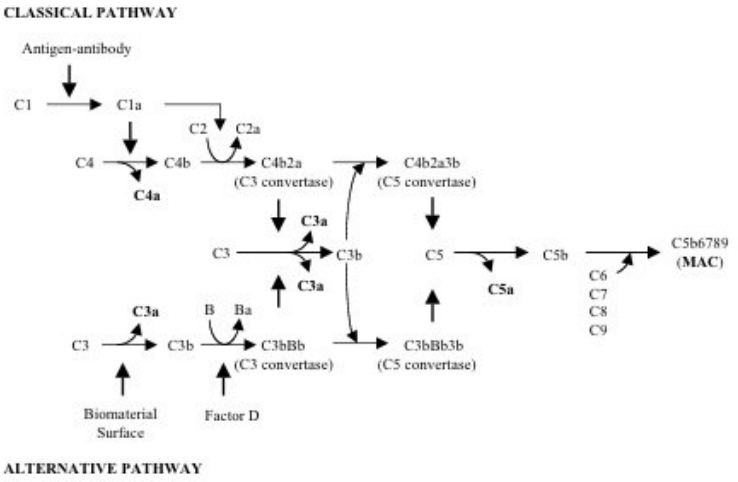

Figure 3.5 Simplified schematics of the complement system.

The blood coagulation system is designed to hinder bleeding from damaged blood vessels but can also be triggered by artificial surfaces in contact with blood. This system is the second step in the important defense mechanism termed haemostasis. Coagulation means platelet aggregation (primary haemostasis) and the formation of a fibrin clot (secondary haemostasis). Two separate pathways of the secondary haemostasis are distinguished and the clotting cascade may be initialized upon vascular injury (extrinsic pathway) or when contact between blood and a negatively charged foreign material occurs (intrinsic pathway or contact activation). Contact activation is a complex process involving both protein-protein and protein-surface interactions. Four contact factors are attracted to the surface when plasma is exposed to a negatively charged surface, factor XII, factor XI, prekallikrein and high molecular weight kininogen (HMWK), and complexes of these adsorb to the surface. The cascade is believed to start by a spontaneous adsorption of factor XII, followed by spontaneous activation to factor XIIa, which in turn cleaves prekallikrein to release kallikrein and factor XI to form factor XIa. Both prekallikrein and factor XI are transported to the negative surface in a bimolecular complex with HMWK.

In paper IV, carbon and CN_x-films were exposed to human blood plasma and then to anti-bodies towards fibrinogen, HMWK and C3c as shown in Figure 3.6. The complexity of the complement and coagulation cascades makes the interpretation of

these kinds of studies somewhat intricate. However, one can in general say that a high level of a-HMWK indicates that the intrinsic pathway of coagulation is triggered. A high level of a-C3c indicates that C3b is bound to the surface and the complement system may be triggered. The presence of C3b on a surface may, however not necessarily, result in the formation of surface located C3- or C5-convertases. Regardless, many cells and especially defense cells possess receptors that bind to C3b and its degradation products, C3c and C3d. If any antibody towards C3 is bound at lower level to a surface after exposure to blood plasma, a-Fib is often bound to a higher level. This is an indication of the possibility to bind platelets onto the interface, and thereby activate the coagulation system [16]. In addition, it is generally assumed that surfaces that adsorb the least amount of plasma proteins support less platelet adhesion and thus exhibit lower tendency for clotting. However, recent studies suggest that the critical determinant of cellular response (e.g. platelet adhesion) to a surface may be the conformational state of the adsorbed protein layer rather than the total amount of adsorbed protein on the surface [31].

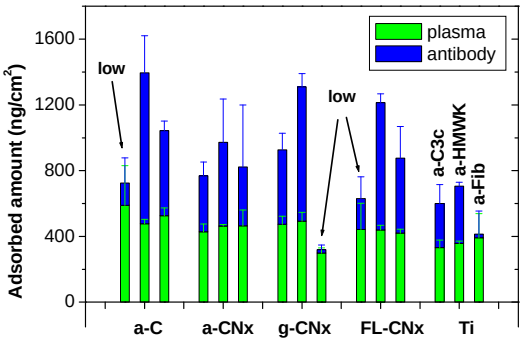

Figure 3.6 Adsorbed surface mass densities after plasma incubation and antibody-incubation of C3c, HMWK and fibrinogen at carbon, CN_x and titanium surfaces.

3.6 Simulated body fluid (SBF)

The formation of bone-like CaP crystals on a surface is a means to test and develop materials intended for integration in bone. Direct bone-implant contact and stem cell differentiation to bone forming osteoblasts is important in order to avoid

development of soft tissue between the implant and bone, leading to micro-movements at the interface, which in turn can lead to wear of the implant material and debris accumulation and a final implant failure [32].

References

[1] Merriam-Webster's Medical Dictionary, Merriam-Webster Inc., 18 May 2009.

[2] Dictionary.com (http://dictionary1.classic.reference.com/browse/macro)

[3] D.F. Williams, Definitions in biomaterials, Proceedings of a consensus conference of the European Society of Biomaterials. Chester, Amsterdam, Elsevier, 1987.

[4] N.A. Peppas, R. Langer, Science, New Series 263 (1994) 1715-1720.

[5] www.realizeband.com/dtcf/pages/glossary.htm

[6] F.Z. Cui, D.J.Li, Surf. Coat. Technol. 131 (2000) 481-487.

[7] S.B. Goodman, R.C. Chin, S.S. Chiou, D.J. Schurman, S.T. Woolson, M.P. Masada, Clin. Orthop. 244 (1989) 182-187.

[8] J. Hong, J. Andersson, K. Nilsson Ekdahl, G. Elgue, N. Axén, R. Larsson, B. Nilsson, Thrombosis and Haemostasis 82 (1999) 58-64.

[9] B. Wälivaara, A. Askendal, I. Lundström, P. Tengvall, J. Biomater. Sci. Polymer Edn. 8 (1996) 41-48.

[10] B.D. Ratner, D.G. Castner, T.A. Horbett, T.J. Lenk, K.B. Lewis, R.J. Rapoza, J. Vac. Sci. Technol. A8 (1990) 2306-2317.

[11] Any book in biochemistry, e.g. Biochemistry, Fifth edition, J.M. Berg, J.L. Tymoczko, L. Stryer, W.H. Freeman and Company, New York.

[12] F.Z. Cui, D.J. Li, Surf. Coat. Technol. 131 (2000) 481-487.

[13] B.D. Ratner, A.S. Hoffman, F.J. Schoen, J.E. Lemons (Eds.), Biomaterials Science, Elsevier Academic Press, San Diego 2004, Chapter 3.2.

[14] M.W. Mosesson, J. Thromb. Haem. 3 (2005) 1894-1904.

[15] C.E. Hall, H.S. Slayter, J. Biophys. Biochem. Cytol. 5 (1959) 11.

[16] T. Horbett, J.L. Brash (Eds.), Proteins and Interfaces II, ACS Symposium series 602, American Chemical Society, Washington DC, 1995, Chapter 5.

[17] R.A. Burton, G. Tsurupa, L. Medved, N. Tjandra, Biochemistry 45 (2006) 2257-2266.

[18] L. Tang, J.W. Eaton, Molecular Medicine 5 (1999) 351-358.

[19] E. Leber, University of Washington Engineered Biomaterials (http://www.uweb.engr.washington.edu/research/tutorials/proteinadsorbtion.html)

[20] M.W. Mosesson, R.F. Doolittle (Eds.), Molecular Biology of Fibrinogen and Fibrin, Annals of the New York Academy of Sciences, 408, New York Academy of Sciences, New York, 1983, p. 131.

[21] www.albumin.org

[22] W. Norde, Coll. Surf. B: Biointerfaces 61 (2008) 1–9.

[23] J.D. Andrade, V. Hlady, Adv. Polym. Sci. 79 (1986) 1-63.

[24] H. Elwing, Biomaterials 19 (1998) 397-406.

[25] S. Tunc, M.F. Maitz, G. Steiner, L. Vázquez, M.T. Pham, R. Salzer, Coll. Surf. B: Biointerfaces 42 (2005) 219–225.

[26] L.H.H. Olde Damink, P.J. Dijkstra, M.J.A. van Luyn, P.B. van Wachem, P. Nieuwenhuis, J. Feijen, Biomaterials 17 (1996) 765-773.

[27] B. Liedberg, C. Nylander, I. Lundström, Biosensors & Bioelectronics 10 (1995) i-ix.

[28] B. Ivarsson, I. Lundström, Crit. Rev. Biocomp. 1 (1986) 1-96.

[29] K. Tiefenthaler, W. Lukosz, J. Opt. Soc. Am. B 6 (1989) 209-220.

[30] S.M. Kelly, N.C. Price, Curr. Prot. Pept. Science I (2000) 349-384.

[31] B. Sivaraman, K.P. Fears, R.A. Latour, Langmuir 25 (2009) 3050-3056.

[32] S.E. Rodil, “Biocompatibility, cytotoxicity and bioactivity”, G. Messina, S. Santangelo (Eds.), Carbon, Topics in Applied Physics, Springer-Verlag, Berlin, 2006.

Chapter 4

Ellipsometry

Ellipsometry is a technique for optical and microstructural characterization of surfaces, interfaces and thin films. The principle was first described by Drude already in 1889 and the first instrument was built by Rothen in 1945 [1-3]. In this work ellipsometry has been used for optical characterization of a-C and CN_x films, and for in situ monitoring of protein adsorption on the same types of films as well as on silicon.

4.1 Basic theory

In *reflection*-based ellipsometry, which is the most common mode of ellipsometry measurements, the *polarization change* of light due to *reflection* from a surface is measured. The change in polarization is dependent on the properties of the sample including its overlayers. The state of polarization of incident and reflected light can be expressed as

$$\chi_i = \frac{E_p^i}{E_s^i}$$

$$\chi_r = \frac{E_p^r}{E_s^r}$$

where s and p stand for perpendicularly and parallel polarized components of the light relative to the plane of incidence and E_p and E_s are the complex-valued

representations of the electric field. Superscripts *i* and *r* indicates incident and reflected light, respectively. The complex reflectance ratio ρ, which is the basic ellipsometric quantity, is

$$\rho = \frac{\chi_r}{\chi_i} \qquad (4.1)$$

If the sample is isotropic, ρ can, with the above equations, be expressed as

$$\rho = \frac{E_{rp}}{E_{rs}}\frac{E_{is}}{E_{ip}} = \frac{r_p}{r_s} = \tan\Psi e^{i\Delta} \qquad (4.2)$$

where r_p and r_s are the complex-valued reflection coefficients and Ψ and Δ are the *ellipsometric angles*, the quantities that are practically measured with an ellipsometer. Tan Ψ is the ratio between the change in amplitude of the p- and s-components of the incident wave and Δ is the reflection induced change in phase difference between p- and s-components. In Figure 4.1, the ellipsometric principle is shown schematically.

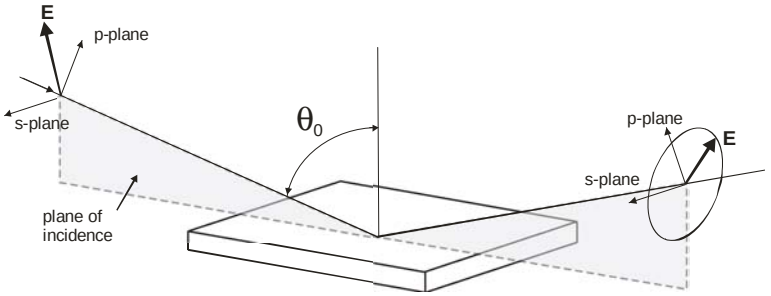

Figure 4.1 Schematic illustration of the ellipsometric principle.

The reflection (and transmission) of a plane electromagnetic wave on a planar interface between two materials (ambient and surface to be examined) can be related to the materials properties by the *Fresnel expressions* (here only the reflection expressions are presented)

$$r_p = \frac{E_{rp}}{E_{ip}} = \frac{N_1\cos\theta_0 - N_0\cos\theta_1}{N_1\cos\theta_0 + N_0\cos\theta_1} \qquad (4.3)$$

$$r_s = \frac{E_{rs}}{E_{is}} = \frac{N_0\cos\theta_0 - N_1\cos\theta_1}{N_0\cos\theta_0 + N_1\cos\theta_1} \qquad (4.4)$$

where θ_0 and θ_1 is the angle of incidence and refraction, respectively, see Figure 4.2.

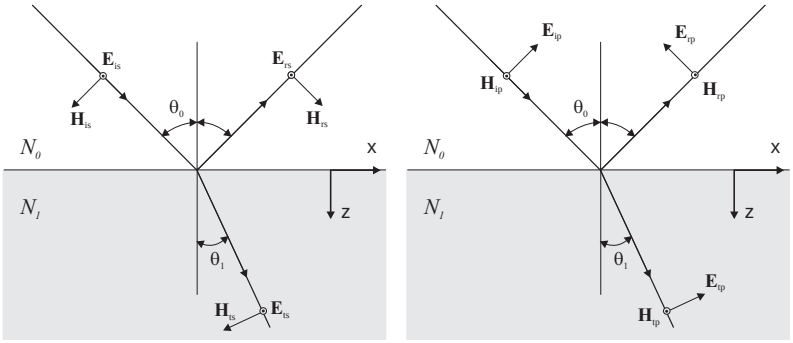

a) b)

Figure 4.2 The s- (a) and p-components (b) of polarized light incident, reflected and transmitted at a planar interface. N_0 and N_1 is the complex refractive index of the ambient medium and substrate, respectively. θ_0 and θ_1 are the angles of incidence and refraction, respectively.

From these expressions the *complex valued refractive index* $N_1=n_1+ik_1$ of the substrate can be extracted, where n_1 is the real part of the refractive index and k_1 is the extinction coefficient. N_1 and the dielectric function ε are related through $\varepsilon = N_1^2$. For layered structures, that means when e.g. a film with thickness d on a substrate is involved, a three-phase system (ambient-film-substrate) must be considered (Figure 4.3). An overall reflection coefficient can then be written as a function of the Fresnel coefficients for the different interfaces as

$$R_p = \frac{r_{01p} + r_{12p}e^{i2\beta}}{1 + r_{01p}r_{12p}e^{i2\beta}} \qquad (4.5)$$

$$R_s = \frac{r_{01s} + r_{12s}e^{i2\beta}}{1 + r_{01s}r_{12s}e^{i2\beta}} \qquad (4.6)$$

where

$$r_{01p} = \frac{N_1\cos\theta_0 - N_0\cos\theta_1}{N_1\cos\theta_0 + N_0\cos\theta_1}. \qquad (4.7)$$

and corresponding expressions for r_{12p}, r_{01s} and r_{12s} are used. In Eqs. (4.5) and (4.6) the film phase thickness is given by

$$\beta = \frac{2\pi d}{\lambda} N_1\cos\theta_1 \qquad (4.8)$$

In the three-phase model, the ellipsometric angles Ψ and Δ are then related to the refractive indices of the three materials and the film thickness through the relation in

Eq. (4.2) with the difference that R_p and R_s from Eqs. (4.5) and (4.6) are used instead of r_p and r_s. The unknown parameters are in most cases d and N_1 and are obtained by regression analysis as briefly described in section 4.6 below.

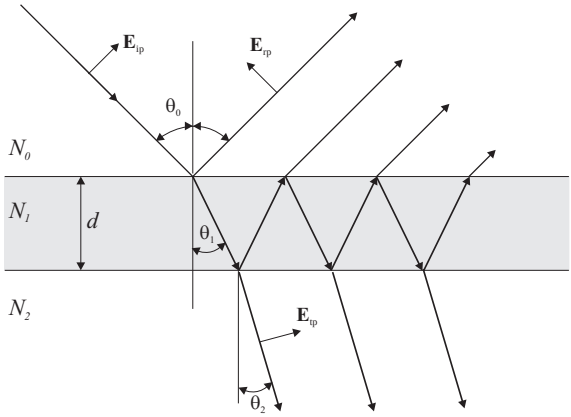

Figure 4.3 The three-phase model for an ambient-film-substrate system with the electric field components in the p-direction shown.

Further details about ellipsometric theory can be found in reference [4].

4.2 Ellipsometric measurement principles

There are three different configurations in ***standard ellipsometry:*** the *external reflection* mode (described in the previous section), the *internal reflection* mode and the *transmission* mode. In internal reflection mode the light is incident at an interface from a medium with a larger refractive index to a medium with a smaller refractive index. At the critical angle the light will be refracted along the interface between the two media. If the angle of the incident light is larger than the critical angle, the light will be totally reflected back into the first medium. Part of the light will, however, still penetrate the first medium due to the evanescent field present in the interface. This phenomenon is used not only in total internal reflection ellipsometry (TIRE) but also in SPR [5]. In transmission ellipsometry the same principle of the incident and transmitted beams of light is used as the principle used for the incident and reflected beams in external reflection ellipsometry.

For isotropic samples as well as for anisotropic samples with diagonal Jones matrices[1] standard ellipsometry is applicable. When the sample is anisotropic and the off-diagonal elements in the Jones matrix are non-zero, ***generalized ellipsometry*** is necessary which includes measurements of at least three polarization changes and three different polarization states of the light beam.

Mueller matrix ellipsometry is a third measurement principle that has to be used when the sample is depolarizing. The state of polarization (unpolarized or partially polarized) of the light is described by a Stokes vector and a Mueller matrix describes the reflection properties of the sample. This is a powerful measurement technique for anisotropic materials with complicated structures.

4.3 Measurement modes and ellipsometer systems

Depending on hardware configuration of the ellipsometer system, several measurement modes are possible for each of the ellipsometric principles described above. All modes of ellipsometry include a light source and a detector, and the optical components in-between, a polarization state generator, a sample stage and a polarization state detector define the measurement mode. Ellipsometer systems may also be divided in compensating/null ellipsometer systems and non-compensating/photometric systems [6]. The most common modes and ellipsometer systems are described in short below.

The most common *null ellipsometer* (NE) consists of a polarizer and a retarder providing elliptically polarized light, which after incidence on a sample surface becomes linearly polarized before it enters a final polarizer (called analyzer). This is referred to as a *PCSA system* and is shown in Figure 4.4.

[1] The Jones matrix was described by C. Jones and represents sample reflection in terms of a matrix, $R = \begin{pmatrix} R_p & 0 \\ 0 & R_s \end{pmatrix}$. If a sample not is isotropic, the off-diagonal elements can be nonzero.

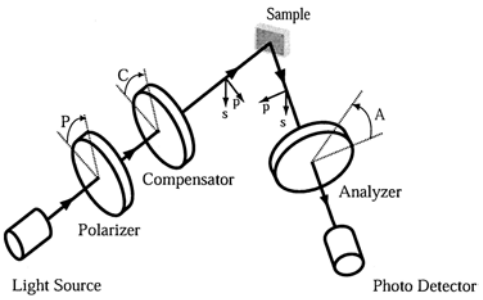

Figure 4.4 A PCSA ellipsometer system used in null ellipsometry. From reference [7]

By changing the angle of the polarizer, the degree of "ellipticity" of the light before it is reflected on the sample, can be adjusted until the "ellipticity" created by the compensator is matched by the polarizing effect of the surface. In this way linearly polarized light is restored after reflection. The angle of the linearly polarized light obtained after reflection, can then be determined by rotating the second polarizer called the analyzer, until extinction is achieved. The angles of the polarizer (P) and analyzer (A) at which a minimum of light passes trough to the detector, are called the ellipsometric nulling angles from which Ψ and Δ are obtained. Monochromatic light, commonly a He-Ne laser is used as light source in this system. Null ellipsometers are frequently used in biological applications such as adsorption studies. In Paper IV this system was used for evaluation of incubations of samples in blood plasma and antibody solutions.

The *rotating-analyzer system* (RAE) is as the name reveals equipped with a rotating analyzer. The light, normally from a white light source, such as a xenon lamp, passes through a monochromator and a polarizer before it is reflected onto the sample surface. This RAE technique is in this thesis referred to as *spectroscopic ellipsometry* (SE). The state of polarization before reflection (normally) is linear and the state of polarization after reflection is generally elliptic and is measured by a rotating analyzer (which is in fact is a polarizer). A polarizer, a sample and an analyzer makes this system which also is called a *PSA* ellipsometer. Sometimes a compensator is used after the polarizer in order to improve the results when measuring on dielectric samples. With the compensator the incident light becomes elliptically polarized and low resolution when measuring on a dielectric sample can be avoided. This RAE technique is in this thesis referred to as *spectroscopic ellipsometry* (SE) with

wavelengths typically in the range 200-2500 nm. If the angle of incidence is made adjustable, multiple angles can be measured and the system is then called a *variable angle spectroscopic ellipsometer* (VASE). This type of system was used in Papers III-V.

If a rotating compensator is added to a PSA system and placed before the analyzer the system is called a PSC_rA system. The analyzer is then not rotating. This type of system is more complex and can be used for generalized ellipsometry. For details, the reader is referred to reference [8]. A PSC_rA system does not have the disadvantage of low resolution for a dielectric sample. A PSC_rA system with the wavelength range 2-30 µm was used in Paper III.

If the ellipsometric parameters are measured versus time, the method is referred to as *dynamic* or *kinetic* ellipsometry. This is performed for *in situ* monitoring of the protein adsorption in Paper IV and V.

4.4 *In situ* measurements of protein adsorption

A variable angle spectroscopic ellipsometer (VASE) from J.A. Woollam Co., Inc. was used for *in situ* measurements of protein adsorption in Papers IV and V using an angle of incidence of 68° and a spectral range of 350–1050 nm. A glass cell with a magnetic stirrer and a flow system for rinsing was used. The set-up is shown in Figure 4.5.

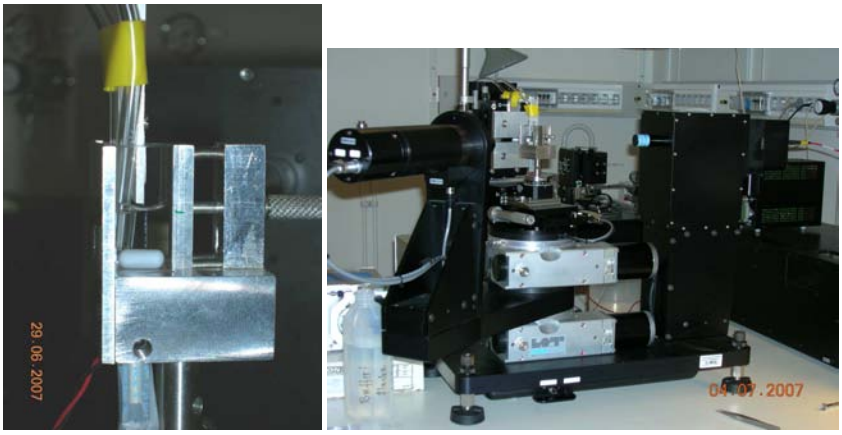

Figure 4.5 a) Set-up for in situ monitoring of protein adsorption used in Paper IV and V. b) The VASE instrument with glass cell mounted on the stage.

4.4.1 What is measured?

Numerous of ellipsometric studies of the dynamics of protein adsorption have been presented [9-11]. However, in most cases the separation of the refractive index *n* and the thickness *d* of a layer is not possible due to that only single wavelength data are available. The ellipsometric data are then mainly sensitive to the optical mass *nd*. An attempt to separate *n* and *d* often fails due to their strong correlation and one resorts to assume a value on *n* whereby a value on *d* can be determined. The thickness obtained in this way is then a fictitious parameter and its value depends on the index chosen. In many cases also the surface mass density Γ is calculated using de Feijters formula [12]. These approaches are sufficient if only the dynamics of adsorption is of interest. However, structural details are lost as these are contained in the layer density and the layer extension into the solvent. The layer density is obtained from *n* and can vary from very low values, whereby *n* is close to the value of the solvent, to a maximum value equal to the protein volume density, whereby *n* corresponds to the intrinsic value of a compact protein material. If an index corresponding to the intrinsic index of the protein is chosen in the evaluation, the thickness obtained is the thickness the layer would have if it collapses and becomes dense.

The intrinsic index is seldom known but a good approximation should be the refractive index measured for a dense protein layer on a surface in air [13]. The layer extension is defined as the maximum distance from the surface at which protein is found. For a dense protein layer, thickness and extension are the same, but for a density deficient (porous) layer, the (fictitious) thickness is always less than the extension.

In the work presented in this thesis, spectral ellipsometric data are available and a separation of *n* and *d* is possible. Due to that a protein layer may exhibit both in-plane and out-of-plane density variations, the obtained value on *d* neither represents the collapsed thickness nor the true extension but we consider the value to be close to the extension. The value of *n* represents an effective value of the layer index from which density information is accessible.

The refractive index of a protein layer gives information about compactness and hydration of the layer whereas the thickness relates to molecular dimensions and orientations of the adsorbed protein molecules.

4.6 Analyses

The optical properties of the measured sample can not directly be calculated from the ellipsometric angles Ψ and Δ and therefore ellipsometry is an indirect method. Instead, an optical model of the sample under investigation is created and a numerical analysis must be performed. Parameters in the optical model are fitted to experimental data using non-linear regression such as the Levenberg-Marquardt (LM) algorithm, which is an iterative technique that locates the minimum of a function that is expressed as the sum of squares of nonlinear functions [14,15]. It has become a standard technique for nonlinear least-squares problems.

The Cauchy dispersion model has been used in two studies in this thesis. In this model n is given by

$$n = A + \frac{B}{\lambda^2} + \frac{C}{\lambda^4}$$

where A, B and C are fitting parameters and λ is the wavelength. In addition, a multi-sample fitting procedure [16] was performed in Paper IV in order to decrease the correlation between n and d in the protein films on the different CN_x samples.

In the studies of the a-C and CN_x films in this thesis, more advanced dispersion models based on Lorentz oscillators are used. These models are described in more detail in Paper III.

References

[1] P. Drude, Ann. Phys. Chemie 32 (1887) 584.

[2] P. Drude, Ann. Phys. Chemie 34 (1888) 489.

[3] A. Rothen, Rev. Sci. Instr. 16 (1945) 26-30.

[4] R.M.A. Azzam, N.M. Bashara, Ellipsometry and Polarized Light, Elsevier Science B.V., Amsterdam, The Netherlands, 1987.

[5] M. Poksinski, "*Total internal reflection ellipsometry*", Dissertation No. 966, Linköping University, Linköping, Sweden, 2005.

[6] H. G. Tompkins, E. A. Irene (Eds.) Handbook of ellipsometry, Springer Science & Business, 2005.

[7] G. Wang, H. Arwin, R. Jansson, IEEE Sensors J. 3 (2003) 739-743.

[8] R.W. Collins, I. An, J. Lee, J.A. Zapien, “Multichannel Ellipsometry”, Chapter 7 in Ref. [6].

[9] B.J. Tarasevich, S. Lea, W. Bernt, M. Engelhard, W. J. Shaw, J. Phys. Chem. B 113 (2009) 1833-1842.

[10] Y. Samoshina, T. Nylander, P. Claesson, K. Schille´n, I. Iliopoulos, B. Lindman, Langmuir 21 (2005) 2855-2864.

[11] B. Lassen, M. Malmsten, J. Colloid Interface Sci. 180 (1996) 339-349.

[12] J.A. de Feijter, J. Benjamins, F.A. Veer, Biopolymers, 17 (1978) 1759-1801.

[13] H. Arwin, J. Mårtensson, I. Lundström, Appl. Phys. Comm. 11 (1992) 41-48.

[14] K. Levenberg, Quarterly of Applied Mathematics, 2 (1944)164–168.

[15] D.W. Marquardt, SIAM Journal of Applied Mathematics, 11 (1963) 431–441.

[16] K. Järrendahl, H. Arwin, Thin Solid films 313-314 (1998) 114-118.

Chapter 5

Summary of the papers

5.1 Paper I

- The aim of the study was:

i) to explore a low substrate-temperature growth process for Si-C-N films by magnetron sputtering

ii) to investigate the role of silicon introduction into CN_x films

iii) to explore if a low surface-energy material can be grown with preserved high hardness

- Method

A series of Si-C-N films were prepared by co-sputtering of Si and C targets in mixed Ar/N_2 atmosphere at substrate temperatures T_s=100, 350 and 700°C, after which the microstructure, hardness and wetting properties of the films were analyzed.

- Results

The Si-C-N films exhibited a textured, amorphous-to-graphite-like microstructure. Films containing more than 12 at.% of Si contained crystallites, 2 - 20 nm in diameter, widely dispersed in an otherwise amorphous matrix. The incorporation of a few at.% Si resulted in a dramatic reduction of the film surface energy compared to pure CN_x films. Contact angles close to the values for Teflon were obtained, i.e. higher values than was reported for Si-containing DLC films. The hardness values of the silicon containing CN_x-films were observed to increase with Si-content. However,

films with lower Si content showed lower hardness values compared to CN_x without Si.

5.2 Paper II

- The aim of the study was:

i) to perform theoretical calculations of the effects of incorporating lattice defects like pentagons and heptagons for BCN compared to BN structures

ii) to investigate the BCN ternary regarding composition, microstructure and mechanical properties (hardness and elasticity)

- Method

A series of B-C-N films were prepared by co-sputtering of B_4C and C targets. Composition, microstructure and mechanical properties of the films were analyzed using RBS, SEM, HRTEM and nanoindentation. The microstructure formation was compared at the atomic level with density functional theory (DFT) calculations.

- Results

Isostructural films were grown with widely varied compositions within the B-C-N ternary system. Similar to CN_x films, the ternary $B_xC_yN_z$ compounds exhibited a dense fullerene-like microstructure with curved and buckled basal planes that results in a hard material which, at the same time, displays an extremely elastic response. Fullerene-like BC:N films could be grown at a lower temperature compared to what is required for CN_x films. Results from theoretical calculations showed that the presence of carbon in a BN system dramatically lowers the formation energy of curved defects such as the pentagon and the heptagon rings. The finding was fully consistent with the microstructure of BCN films exhibiting longer continuous basal planes compared to a CN_x film.

5.3 Paper III

- The aim of the study was:

i) to determine and analyze optical properties of amorphous carbon, amorphous, graphitic and fullerene-like carbon nitride thin films in the UV-VIS-NIR and IR spectral ranges. SE-data containing quantitative structural information, especially

in the IR and NIR regions (below 8000 cm^{-1} or 1 eV), are rarely available in the literature.

ii) to find correlations between results from XPS, HRTEM and SE.

- Method

Thin films of CN_x and carbon were characterized regarding microstructure and optical properties using XPS, HRTEM and SE.

- Results

Between eight and eleven resonances were observed and modeled in the ellipsometrically determined optical spectra of the films. All films showed strong resonances for C-C (in a-C), C=C or C=N modes, which for the CN_x films most probably is originating from sp^2 C-N bonds, either as N substituted in a graphite site and/or as N bonded in a pyridine-like manner. A $\pi \rightarrow \pi^*$ electronic transition associated with sp^2 C or sp^2 N (N in a pyridine-like configuration) bonds was also present for all films. Several new features were also observed in the ellipsometric spectra. These have not been presented elsewhere and remain so far unidentified.

The correlation of results from XPS, HRTEM and SE of the films in this paper was to a high extent satisfying, finding the correlation between HRTEM and SE of the bending and cross-linking of graphene sheets, as well as the correlation between XPS and SE for the bondings associated with $\pi \rightarrow \pi^*$ transitions and C=N modes. The nitrile contents were not as well correlated whereas the N-H and O-H bonding are not possible to identify with neither XPS nor HRTEM.

Experimental SE-data of all films in the study are presented as the complex dielectric function in the energy ranges 0.07-0.8 eV and 1.0-6.0 eV in Figure 5.1.

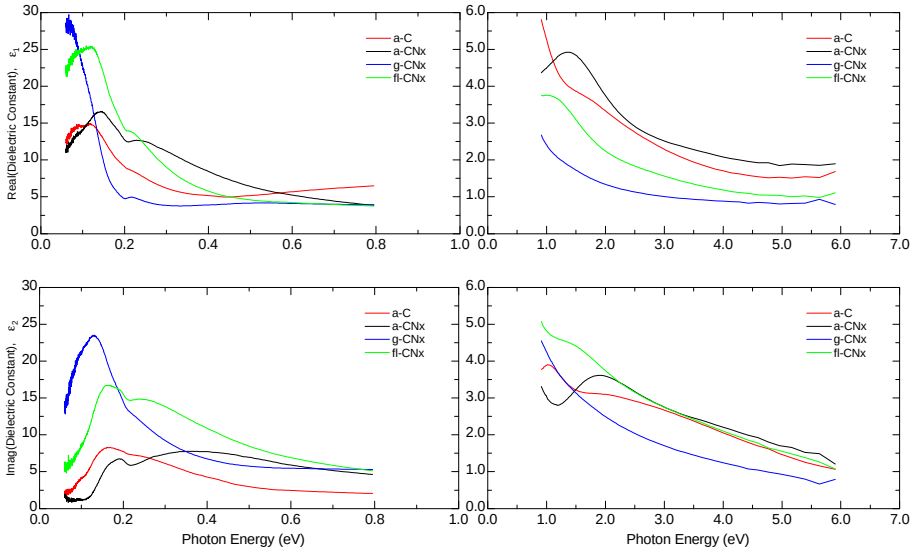

Figure 5.1 Pseudo-dielectric function versus photon energy in the IR and UV-Vis - NIR spectral ranges of CN_x (black, blue and green lines for a-, g- and FL- CN_x, respectively) and amorphous carbon (red line) films. The low energy range (0.07-0.8 eV) is shown to the left and the high energy range (1.0-6.0 eV) to the right with ε_1-spectra on top and ε_2-spectra below.

5.4 Paper IV

- The aim of the study was:

i) to reveal if carbon and CN_x films start the blood coagulation cascade and/or trigger the immune system when exposed to body fluids

- Method

Carbon and CN_x films (the same films as in Paper III) were exposed to human serum albumin, human blood plasma and antibody solutions of factor C3c, HMWK and fibrinogen. The adsorption of HSA was monitored and followed dynamically *in situ* using ellipsometry. Studies of blood plasma and antibody incubations were performed *in situ* using null ellipsometry.

- Results

The carbon and CN_x films adsorbed different amounts of HSA, with higher adsorption observed on the amorphous structures. Indications of surface response to

blood coagulation, complement activation and clotting were observed after incubations in human blood plasma and antibody solutions. All carbon and CN_x films activated the intrinsic pathway of coagulation, indicating a negative surface charge at physiological conditions. The amorphous carbon and graphitic films indicated to be more activating than the other films, especially compared to the a-CN_x film.

The results indicate that the a-C and FL-CN_x films may have a future in soft tissue applications due to their low immuno complement deposition, whereas the g-CN_x is a possible bone replacement candidate. The a-CN_x film shows a remarkably complex and high bioactivity and the g-CN_x film shows a high bioactivity as compared to a titanium reference. Bone-like bioactivity of the carbon and CN_x films were tested using simulated body fluid (SBF) with an ion concentration and pH equal to that of human blood plasma. In Figure 5.2 the evolution of calcium phosphate crystals on the a-CN_x film is observed.

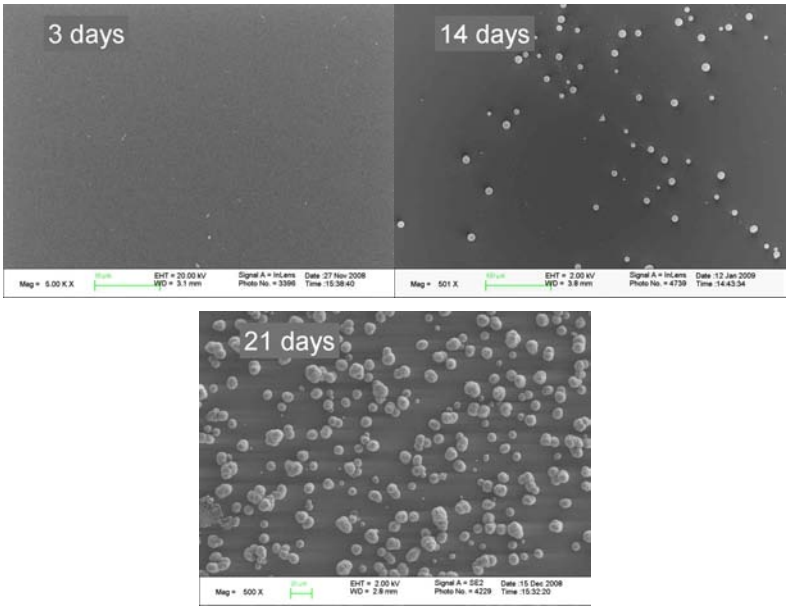

Figure 5.2 SEM observations of the formation of calcium phosphate crystals on a-CN_x after 3, 14 and 21 days in SBF.

Further studies are required to be able to say anything specifically about the use of these materials in a biological environment. However, the indications of their biological interactions are promising.

5.5 Paper V

- The aim of the study was:

i) to find a preparation technique for formation of thick protein layers

ii) to develop an ellipsometric methodology to quantitatively determine the protein matrix surface mass density, refractive index and thickness.

iii) to add some understanding in how the structure of a protein layer evolves as adsorption on a surface proceeds.

iiii) to perform a pilot study for incorporation of a drug into a protein matrix for drug delivery purposes.

- Method

Fibrinogen molecules were covalently bonded on functionalized silicon surfaces and cross-linked in several incubation steps using an ethyl-3-dimethyl-aminopropyl-carbodiimide and N-hydroxy-succinimide (EDC/NHS) affinity ligand coupling chemistry. The growth of the structure was followed *in situ* using dynamic ellipsometry and characterized at steady-state with spectroscopic ellipsometry. The growth was also compared with earlier work on *ex situ* growth of fibrinogen multilayers studied by single wavelength ellipsometry.

- Results

The first Fib incubation step of the experiments produced a layer that was thicker than a monolayer indicating an adsorption process with a complicated molecular organization with a mixed set-up of molecular interactions. The first Fib layer was in all experiments of the order of 40 nm which was much larger than the thickness-increase due to the second, third and fourth Fib incubations. Experimental dynamic data recorded during incubation and rinsing of the first Fib and EDC/NHS layers for one of the multilayer experiments can be viewed in Figure 5.3.

Contributions to the development of a model for layered growth of fibrinogen have hopefully been provided. It is suggested that a mixture of covalent bonds (both N-terminally and other amines) and hydrophobic interactions are involved in the adsorption of fibrinogen molecules.

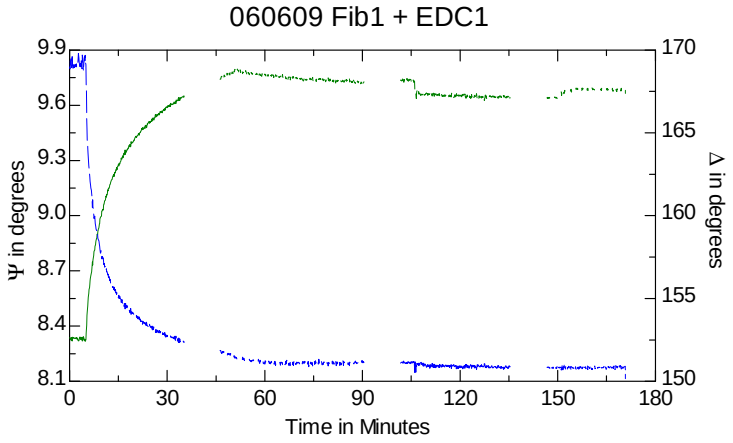

Figure 5.3 Dynamics recorded during incubation and rinsing of the first Fib and EDC/NHS layers for one of the multilayer experiments. The increasing curve (moving from the left) represents Ψ and the decreasing curve represents Δ.

5.6 Paper VI

- The aim of the study was:

i) to explore the effects of ion and protein concentration on refractive indices of fluids

- Method

The minimum deviation technique was used to measure how the wavelength dependent refractive index of a solution depends on its ion and protein concentration.

- Results

In this work we point out the importance of using the correct spectral refractive index data of the fluid when analyzing ellipsometric data from protein adsorption studies. Simulations showed that thickness values of protein layers can have errors in the order of 30% if the solution index deviates 0.001. Ions in fluids of physiological strength influence the refractive index in the 3rd decimal. Protein molecules influence the refractive index in the 4th decimal up to 1 mg/ml and in the 3rd decimal for higher concentrations. Figure 5.4 shows the refractive index versus ion concentration of phosphate buffered saline (PBS) at a few selected photon energies.

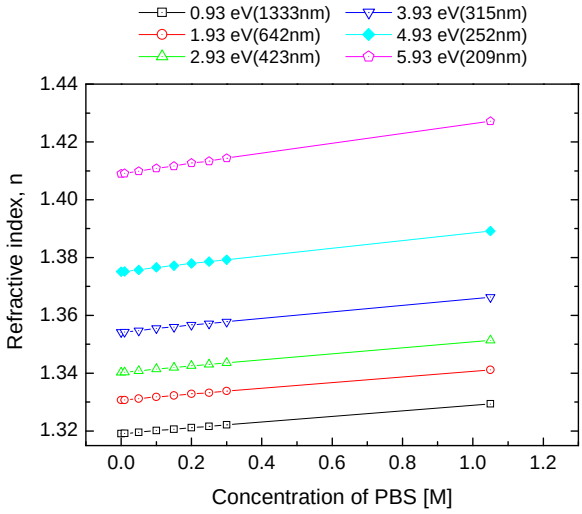

Figure 5.4 Refractive index versus ion concentration of PBS for a selected number of photon energies.

Acknowledgements

The course of my studies has been filled with joy and adventures, but also hard times followed me. Some things you just cannot rule… That applies for both science and life itself and perhaps exactly that is what makes the tumbling and mischief during the search for the truth worth living for, some things simply can not be controlled.

I would like to express my sincere gratitude to ALL the people I have met during these years and hopefully we will meet some time again!

There are some people that I especially have to mention though…

Hans Arwin, my supervisor, for opening the door to the model world and giving me the opportunity to take a step into the 'protein science field'. Thank you for extensive reading of the manuscripts during the last trembling days and for your support and great enthusiasm, both in the lab and outside the walls of hard work. You are the most humble professor I have met, and I appreciate you for that.

Pentti Tengvall, my co-supervisor, for lending me your time to try to explain the complexity of the processes in the human body and for giving me some insights in a new area of science. Thank you for being enthusiastic and for reading the manuscripts.

Lars Hultman, my co-supervisor, for your support and guidance during the first years as my supervisor and for letting me continue in the research field of carbon nitride. You are a great preserver of the use of the English and Swedish languages.

Göran Hansson and *Louise Rydström* at IFM, for making it possible for single mothers to perform doctoral studies at the department. Thank you for great support during this time.

Stefan Klintström for being the most excellent guide for all the PhD students in Forum Scientium, and for great explanation of the biochemical secrets.

Susann Årnfelt, for a couple of hectic but very nice weeks in Nebraska, in November 2005. Starbucks and bananas helped us survive! Thank you also for being helpful with small and big issues regarding administration.

John Woollam, for making the stay in Lincoln very comfortable and a very nice memory.

Co-workers in the early work: *Niklas, Mats, Esteban, Zsolt* and all the nice people in the *Thin Film Group.* We had a great time!

Co-workers in the late work: *Michal, Jimmy, Kenneth, Roger, Christina, Arturo, Saby, Greg, Dan, Andrej* and *Jörg*. Without you it would not have been as nice to go to work all these days.

Agneta Askendal, for sharing your skills in the laboratory.

Thomas Lingefelt and *Kalle Brolin*, for always being positive and in addition very helpful with microscopes and pumps.

The TFE-people: *Per, Mats, Chun-Xia, Erik, Kenneth, Mikael, Anne-Marie, Sofia, Grzegorz, Helena, Sven, Rickard, Eva* and *the rest*.

A few of you have understood my situation during the last years and I want to thank you for being there.

Ann-Charlotte o Peter för att ni alltid har ställt upp med en hjälpande hand, oavsett hur upptagna ni själva än varit och för att ni öppnat ert hem för både Tove och mig! *Ann-Kristine o Kenneth* för god mat, hjälp med flytt, och för att man alltid känner sig välkommen hem till er!

Alla trevliga människor och hästar i *Heda Ridklubb*, ni har verkligen lyst upp min tillvaro och hjälpt mig koppla av! Ett särskilt tack till *Berit, Jennifer och Hannah* för att ni avlastat mig och stöttat och hjälpt Tove när jag inte riktigt hunnit med. Och Tack *Tove* för att du delar hästintresset med mig!

Mina vänner, särskilt *Eva* och *Susanne* - tack för att ni har peppat mig eller "tagit ner mig på jorden" när det behövts.

Alla vänner som jag inte hört av mig till på länge, jag tänker på er allt som oftast. Hoppas jag nu ska få tid och ork att återuppta kontakten med er.

Min älskade *familj*, jag skulle vara intet utan er!
Ett särskilt tack till *Mamma* för ALL hjälp genom åren, med allt från hundvakt till markservice och möjlighet till underbara vistelser i Fyrudden. Utan dig hade detta inte gått vägen. Jag älskar dig, det vet du!

Mina systrar, *Anna* och *Camilla*, som båda betyder väldigt mycket för mig och som har hjälpt mig på många sätt genom åren. *Era familjer*, som faktiskt känns som mina också.

Axel, för att du släppt iväg mamma när hon behövts i Linköping och för att du stått ut med Trixa trots ditt svala intresse för hundar. Tack också för att du ledde mig in på "material-vägen".

Pappa, om du ändå hade kunnat stanna hos oss.. Du hade varit mig till stor hjälp med din kunskap och ditt intresse för allt. Jag vet att du är glad för min skull.

Och så då slutligen, *Tove*, ljuset och glädjen i mitt liv. Tack för ditt tålamod, särskilt dessa senaste tre månader. Jag älskar dig såå mycket! Och glöm inte att du kan mycket mer än du tror!

Torun
Linköping i juni 2009

“…
Du går, och ingenting av detta har jag givit dig.
Jag nådde aldrig dit, där ditt väsen ligger bart.
Du går, och ingenting av mig tar du med dig –
lämnar mig åt nederlaget.”

- ur Avsked (För trädets skull) av Karin Boye (1900-1941)

Avsked har varit en av de svåraste sakerna att hantera i mitt liv. Detta avslut är ju också ett slags avsked, men känns dock enbart som början på något nytt, istället för slutet på något trevligt. Även om det har varit det också..